9th French/Belgian OpenFOAM users conference

Book of abstracts



June 3 & 4 2026,
Talence, France

With the support of

I2M BORDEAUX INSTITUT DE MÉCANIQUE ET D'INGÉNIERIE

Arts et Métiers Institute of Technology

université de BORDEAUX

HyFAR - ARA

The open-source LaTeX template, AMCOS_booklet, used to generate this booklet is available at `https://github.com/maximelucas/AMCOS_booklet`

Contents

About **4**
- FOAM-U . . . 4
- The conference . . . 4
- Organizing committee . . . 4
- Awards . . . 4

Timetable **5**
- Wednesday, 3 of June . . . 5
- Thursday, 4 of June . . . 6

List of Abstracts – Talks **7**

List of Posters **22**

Partner Institutions and Sponsors **38**
- Institutions . . . 38
- Sponsors . . . 38

About

FOAM-U

The purpose of our association is to initiate, encourage, and promote the progress and dissemination of techniques, practices, processes, and achievements relating to the use and development of OpenFoam© software.

The conference

The Institute of Mechanics and Mechanical Engineering I2M Bordeaux (UMR CNRS 5295, Université de Bordeaux, Arts et Métiers, Bordeaux INP, INRAE), Foam-Utilisateurs (the French OpenFOAM© users group), and the Belgian OpenFOAM© users group are pleased to invite you to the French/Belgian conference of OpenFOAMő users. For the ninth year in a row, this event aims to bring together OpenFOAM© users and those interested in potential software applications. People from academia and industry are invited to present advances in their relevant research and development fields, exchanging ideas and information in an interdisciplinary environment. This conference will provide an ideal opportunity to develop new collaborations and to meet experts.

Organizing committee

Jean Lachaud	I2M / Université de Bordeaux
Aurélie Louis-Napoléon	R.Tech
David Uystepruyst	Université Polytechnique Hauts-de-France
Yann Recoquillon	Aero Concept Engineering
Victor Pozzobon	CentraleSupélec

Awards

Rachih Azeddine	First poster award
Ramin Raesi	Second poster award
Joanna D'Antoni	Third poster award

Timetable

Wednesday, 3 of June

Session	Time	Duration	Type	Title	Speaker
	8h30	0h30	Welcome	Welcome coffee & Poster installation	
	9h00	0h10	Welcome	Welcome address	Organizing committee
1	9h10	1h00	**Plenary**	**Accurate subface-based finite-volume discretization of diffusion equations over unstructured grid**	**Pierre-Henri Maire**
1	10h10	0h20	Break & Posters	**Poster flash presentations**	**Poster presenters**
	10h30	0h30	Break & Posters	Discussions around posters, with cakes and coffee	
1	11h00	0h20	Regular	VOF SIMULATIONS OF A LIQUID FILM FLOWING OVER A SINGLE PERFORATION	Gamet Lionel
1	11h20	0h20	Regular	Modeling interfacial mass-transfer in gas-agitated reactors	Mishra Rishikesh
1	11h40	0h20	Regular	What's new in ParaView?	Gombert Louis
	12h00	2h00	Break & Posters	Lunch time	
2	14h00	0h20	Regular	Numerical analysis of the forces exerted by submerged landslides on slender cylinders	Barajas Gabriel'
2	14h20	0h20	Regular	Heat transfer modeling in porous media	Begall Moritz
2	14h40	0h20	Regular	From Filtering to Forcing: advanced turbulence modeling via Data Assimilation and Machine Learning	MOUSSIE Tom
2	15h00	0h20	Regular	Modeling Two-Phase Flows Using Efficient Multi-Scale Phase Change Closure Methods: Contact Line Effect	FARHAT Rafa
	15h20	0h40	Break & Posters	Discussions around posters, with cakes and coffee	
3	16h00	0h20	Regular	Incompressiblefoam: a new time consistent framework with bdf and dirk integration schemes	FERRO Paulin
3	16h20	0h20	Regular	Immersed Boundary reconstruction in OpenFOAM	Lorthioir Maxence
3	16h40	0h20	Regular	Implementing multi-region convergence controls	Matveichev Alexey
	17h00	2h00	Social event	Social event (travel and visit)	
	19h00	1h00	Social event	Travel to the diner	
	20h00	–	Social event	Gala diner	

Thursday, 4 of June

Session	Time	Duration	Type	Title	Speaker
	8h30	0h30	Welcome	Welcome coffee	
4	9h00	1h00	**Plenary**	**Fire simulations with OpenFoam**	**Pr. Franck Richard**
4	10h00	0h20	Regular	Modeling of an Atmospheric Re-entry Capsule	Louis-Napoléon Aurélie
4	10h20	0h20	Regular	Advanced prediction of the flow around vortex generators via data assimilation	Heraoua Lakhdar
	10h40	0h40	Break & Posters	Poster flash presentations	
5	11h20	0h20	Regular	Simulation of a Turbulent Wall Flame Using FireFOAM	Fawaz Mohamad
5	11h40	0h20	Regular	Couplage explicite pour la modélisation de lablation des matériaux poreux en rentrée hypersonique	Merlaud Gabriel
5	11h40	0h20	Regular	Image-Based Pore-Scale Investigation of Permeability and Pyrolysis-Induced Morphological Evolution in Wood	M'jikou Abderrahman
	12h00	2h00	Break & Posters	What's new in ParaView?	
6	14h00	0h20	Regular	Thermal Management of Electronic Components: Innovations and Modeling	Salmon Fabien
6	14h20	0h20	Regular	Validation effort of the porous approach implementation in OpenFoam	Prud'homme Florentin
6	14h40	0h20	Regular	Stochastic Modeling of Hydrodynamic Particle Bridging and Permeability Impairment in Pore Networks	Maya Fogouang Laurez
6	15h00	0h20	Regular	Simulation of wood drying, pyrolysis and shrinkage for fire resistance applications.	Penicaud Josselin
	15h20	0h40	Break & Posters	Modeling Two-Phase Flows Using Efficient Multi-Scale Phase Change Closure Methods: Contact Line Effect	
7	15h00	0h20	Regular	Modélisation couplée solide-fluide d'une analyse thermogravimétrique	Trouillet Nell
7	15h20	0h20	Regular	sedExnerFoam: Modeling Sediment Transport and Morphodynamic Evolution	Renaud Matthias
7	16h00	0h20	Regular	Modélisation des protections thermiques pyrolysables avec PATO : analyse de la mission Hayabusa	ZAKARIA Nadim
	16h20	0h40	Break & Posters	Poster prizes awards - Closing address	Organizing committee
	17h00	1h00		FOAM-U general assembly	

List of Abstracts – Talks

VOF SIMULATIONS OF A LIQUID FILM FLOWING OVER A SINGLE PERFORATION

Gamet Lionel, IFP Energies nouvelles

We perform the computation of a flow going down a single-perforated plate with Volume-Of-Fluid methods. Comparison of numerical results using both algebraic and geometric VOF solvers is performed against experimental data.

Modeling interfacial mass-transfer in gas-agitated reactors

Mishra Rishikesh, CentraleSupélec

Modeling of interfacial mass-transfer is a prominent question for chemical engineers. From a CFD perspective, it requires an accurate interplay of five concepts: flow, transport, exchange surface, exchange thermodynamics, and transfer rate. These pieces combine physical intuition with mathematical insights and acknowledgement of ambiguities, closure assumptions, and free parameters. As an example, gas dissolution in gas-stirred reactors will be presented through model studies. We will develop the various aforementioned pieces, as well as their validation. Finally, we will apply the model towards numerical exploration of phenomena which are difficult to estimate directly in a complex flow environment, such as turbulent mass-transfer, and pseudo-turbulence in bubbly flow.

What's new in ParaView?

Gombert Louis, Kitware

In this presentation, we highlight the new features of ParaView 6.0 and 6.1 that came out in the past year. We explore how the user interface has changed to improve the post-processing experience. Then, we show how OpenFOAM is evolving to support new file output formats, in particular VTKHDF, the newer HDF5-based VTK file format, that offers efficient parallel I/O capabilities. Finally, we discuss how the ParaView rendering stack is being improved and standardized with ANARI, and introduce in-progress work regarding WebGPU and WebAssembly integrations.

Numerical analysis of the forces exerted by submerged landslides on slender cylinders

Barajas Gabriel', IHCantabria - Universidad de Cantrabria

OpenFOAMő is used to investigate sudden impacts on slender cylinders caused by granular submerged landslides, capturing the interaction between the granular slide and the free surface, resolving large-scale vortical structures and their role in energy transfer and dissipation. Results highlight two distinct stages of the phenomenon: (i) the initial impact and jet formation, and (ii) turbulent dissipation and recirculation. The analysis provides quantitative and qualitatie insights into velocity fields, pressure distributions, identifying key mechanisms driving energy loss.

Heat transfer modeling in porous media

Begall Moritz, Forschungszentrum Jülich GmbH

Porous media are at the center of many industrial applications involving chemical reactors, where a fluid passes through a solid structure such as a bed of catalyst particles or a metal foam. Modeling the fluid flow and heat transfer in these porous structures is important to understand and predict the performance of the reactors. However, spatially resolving the porous structures can be very computationally challenging and is often not necessary. Instead, using a volume-averaged approach can yield approximate solutions much more efficiently.The momentum loss induced by porous resistance can be modeled in OpenFOAM using a porosity source, e.g., via specifying Darcy-Forchheimer coefficients. Calculating the heat transfer is however more difficult, particularly in the case of local thermal non-equilibrium, and is as yet not natively supported in OpenFOAM. Here we extend existing solvers to accommodate coupled but distinct solid and fluid temperature fields, as well as thermal conductivities and flow resistances that depend on a locally variable porosity field. This enables the efficient simulation of heat transfer in porous media.

From Filtering to Forcing: advanced turbulence modeling via Data Assimilation and Machine Learning

MOUSSIE Tom, Arts et Métiers ParisTech

In the present work, a Multi-Fidelity Ensemble Kalman Filter [Popov et al., 2021] is developed to augment numerical model predictions for the analysis of a realistic industrial configuration, namely a single-stage axial compressor referred to as CME2. In the MFEnKF framework, the low-resolution ensemble members are solved using a RANS model, while high-fidelity simulations consist of hybrid RANS-LES runs. The Multi Fidelity-Data Assimilation (MF-DA) filtering is nourished with observational data obtained via experimental PIV measurements. Although MFEnKF's elegant design is able to reduce the computational burden when compared to classical ensemblistic techniques, such as the EnKF, data mapping in between High Fidelity and Low Fidelity models, large state vectors and the High-Fidelity models costs, still represent a relatively expensive approach, especially if the aim is to deploy DA results for real-time applications.To overcome such difficulties, an Artificial Neural Network (ANN) [Villiers et al., 2025] is integrated with the objective to substitute the action of the MF-DA while decreasing the computational costs and increasing the results accuracy. The ANN is given characteristics inputs from the flow fields with the aim to output forcing terms which directly act onto the discretized Navier-Stokes equations.Flow data from the MF-DA filtering is streamed to the ANN training process from which forcing terms are used to supplant and mimic MFEnKF operations. The method, which will be presented at the workshop, shows excellent results in terms of accuracy vs costs ratio for the case investigated.

Modeling Two-Phase Flows Using Efficient Multi-Scale Phase Change Closure Methods: Contact Line Effect

FARHAT Rafa, PhD student - ISAE ENSMA, Poitiers

The increasing power densities of modern electronics and high-temperature propulsion systems require efficient cooling technologies. Passive two-phase devices, such as thermosyphon loops, were found to possess considerable potential as thermal management systems due to their ability to transfer heat efficiently through phase-change. A thermosyphon loop is defined as a closed system, partially filled with a working fluid, and the rest with its vapor. Heating at the evaporator (hot spot) and cooling at the condenser (cold spot) facilitate fluid circulation by the process of evaporation and condensation. Despite their strong industrial potential, robust and reliable predictive models capable of describing these systems at the device scale remain scarce.The objective of the proposed PhD project is to develop efficient multi-scale numerical models for two-phase flows with phase change using computational fluid dynamics simulations based on a Volume-of-Fluid interface-capturing method combined with the isoAdvector interface method for advecting fluid phases, a less noisy transport algorithm, implemented within the open-source CFD framework OpenFOAM.Although current simulations capture the main thermosyphon flow regimes, they remain limited by computational cost and incomplete modeling of mechanisms. Fully resolving three-dimensional two-phase flows is unfeasible due to both space and time scale discrepancies. In such cases, micro-scale phenomena near the liquidvaporsolid contact line, which are critical for evaporation and heat transfer, are barely considered if at all. Mass conservation in the context of compressible flows and effects such as interface curvature and recoil pressure are also often not considered.The present investigation aims at enhancing the physical modeling of micro-scale phenomena without compromising the system's computational efficiency. This can be achieved through advances in contact-line heat transfer and in modeling separately thin-film evaporation/condensation processes. These developments are expected to improve the predictability and robustness of numerical simulations and help design optimized two-phase cooling devices for future high-power applications.

incompressiblefoam: a new time consistent framework with bdf and dirk integration schemes

FERRO Paulin, SARL G-MET Ingénierie

This work focuses on the development of a new incompressible solver, incompressibleFoam, within OpenFOAM and integrating several numerical methods within the same framework. Two momentum interpolation (NCMI/CMI) methods are implemented, two forms of the pressure Poisson equation (corrected/standard). Regarding time discretization, steady-state, Backward Differentiation Formula (BDF) and the Singly Diagonally Implicit Runge-Kutta (SDIRK) methods, up to the third order, are implemented. The solver is tested on three benchmark cases to assess the performance of different numerical configurations. The results are also compared with the standard incompressible solver of OpenFOAM: pimpleFoam. They provide perspective on previous attempts to improve OpenFOAM incompressible solvers and give practical results regarding the choice of momentum interpolation methods, pressure equation formulations, and time discretization schemes. It is found that the pressure-corrected form should be avoided while using the NCMI and that third order schemes are not superior to 2nd order schemes. The CMI should be privileged to avoid time step and relaxation factor dependence and pressure velocity decoupling. https://github.com/ferrop/incompressibleFoam

Immersed Boundary reconstruction in OpenFOAM

Lorthioir Maxence, ENSAM

Immersed Boundary Methods (IBM) have become a powerful alternative to body-fitted meshes for simulating flows involving complex or moving geometries, particularly in industrial configurations such as turbomachinery. However, their application to flows exhibiting strong gradients of several physical quantities, such as rotating machines, due to challenges in enforcing accurate boundary conditions and the robustness of near-wall reconstructions.This work presents a geometric IBM framework implemented within OpenFOAM, designed for Cartesian meshes and complex immersed geometries. The method relies on a cell-based classification strategy that distinguishes fluid, solid, and interface cells through a mask classification.Using geometric constructions similar to the principles of ghost-cell methods, the approach introduces a reproducible local geometric stencil aligned with the surface normal, enabling the reconstruction of flow quantities at the immersed boundary. Relay points are generated in the fluid region to support standardized interpolation schemes, ensuring consistency with the physical boundary conditions.Results demonstrate that the proposed geometric construction provides a reliable foundation for IBM in OpenFOAM, with particular relevance for industrial applications involving complex geometries and high Reynolds flows.

Implementing multi-region convergence controls

Matveichev Alexey, O2M Solutions

Conjugate heat transfer solvers in OpenFOAM(R) use a fixed number of outer iterations and have no convergence controls. For the numerical study of a cool store, we needed convergence controls to ensure the correct solution. In the talk we present an experience of the implementation of the multi-region solution controls similar to pimpleContol in the CHT family of solvers.

Modeling and Stability Analysis of the KLARA Atmospheric Re-entry Capsule

Louis-Napoléon Aurélie, R.Tech

KLARA is a compact, low-cost atmospheric re-entry capsule designed to collect high-value physical data during the disintegration of a host satellite. Its modular design enables easy integration across multiple platforms, including balloons, sounding rockets, and satellites.The main objective of this project is to model KLARAs atmospheric re-entry to ensure reliable data recovery. This involves the use of various simulation tools covering a wide range of flow regimes, from supersonic to subsonic conditions.Among these tools, OpenFOAM is used to analyze the capsules aerodynamic behavior. Particular attention is given to trajectory stability, which is critical to ensuring the capsules survival during re-entry. Multiple computational analyses are therefore carried out to evaluate its performance and robustness under extreme conditions.

Advanced prediction of the flow around vortex generators via data assimilation

Heraoua Lakhdar, IMT Nord Europe

Mastering and optimizing passive flowcontrol mechanisms is of primary interest for improving the performance of energy systems. Today, advanced experimental measurements and cuttingedge numerical methods make it possible to accurately describe physical phenomenaeven complex onesat the cost of data processing and computational time that are highly energyintensive, making optimization very expensive.In a context of dual carbon constraints (energyclimate), optimized use of digital computing resources is essential. The objective of this study is to propose a methodology for flowcontrol techniques (through vorticity generation), based on both stateoftheart experimental data and the coupling of numerical simulation with combined dataassimilation and machinelearning techniques.Results show that the method successfully couples the high fidelity prediction of experiments with the quasi-continuous description of CFD numerical methods.

Simulation of a Turbulent Wall Flame Using FireFOAM

Fawaz Mohamad, PPRIME/ENSMA

This work presents the numerical simulation of a turbulent wall fire configuration using FireFOAM, inspired by well-documented experimental studies. The objective is to reproduce the main flow and thermal features of the flame in the gas phase as a preliminary step toward future coupling with solid-phase pyrolysis models with PATO.A structured multi-block mesh is employed to capture the near-wall region, the air entrainment zone, and the outer flow. Since the laminar-to-turbulent transition cannot be fully resolved on practical grids, a turbulence forcing strategy is applied by introducing controlled fluctuations in the fuel mass flow rate to promote early transition.The study focuses on the characterization of temperature, velocity, turbulent viscosity, and wall heat flux distributions. Numerical results are analyzed through spatial averaging and compared to available experimental and numerical reference data. Particular attention is given to the decomposition of total heat flux into radiative and convective contributions.The results demonstrate that the main features of the flame structure and heat transfer are reasonably captured. This work constitutes a first step toward more advanced simulations including pyrolysis and solidgas coupling in fire scenarios through the coupling between PATO and FireFOAM.

Couplage explicite pour la modélisation de lablation des matériaux poreux en rentrée hypersonique

Merlaud Gabriel, Univ. Bordeaux, CNRS, Bordeaux INP, I2M, UMR 5295, F-33400 Talence, France

La croissance rapide du nombre dobjets en orbite terrestre rend la désintégration des débris spatiaux lors de la rentrée atmosphérique un enjeu majeur. Dans ce contexte, la conception pour la destruction (design for demise, D4D) suscite un intérêt croissant, notamment au sein de lAgence Spatiale Européenne. Il est donc pertinent détudier la dégradation des débris spatiaux lors de la rentrée atmosphérique, en particulier les phénomènes de fissuration et de fragmentation. Dans ce cadre, un couplage explicite entre PATO, solveur de réponse des matériaux poreux basé sur OpenFOAM, et le solveur découlement hypersonique Eilmer a été développé. La condition de couplage sappuie sur Mutation++ pour modéliser la chimie gazsurface hors équilibre à linterface fluidesolide, en prenant en compte lablation, les transferts de masse, le dégazage pyrolytique et les effets de soufflage, qui influencent fortement le flux thermique et la composition des espèces à linterface. Testée sur des cas hypersoniques représentatifs, cette méthode permet de mieux décrire la dégradation des matériaux à haute température et contribue à améliorer la prédiction de la désintégration des structures spatiales.

Image-Based Pore-Scale Investigation of Permeability and Pyrolysis-Induced Morphological Evolution in Wood

M'jikou Abderrahman, Univ. Bordeaux, CNRS, Bordeaux INP, I2M, UMR 5295, F-33400, Talence, France

Wood pyrolysis induces strong microstructural changes that directly affect gas flow and the evolution of the pore network. This work combines two OpenFOAM-based pore-scale studies to investigate these coupled phenomena in maritime pine. First, image-based CFD simulations performed on synchrotron micro-CT volumes of virgin and pyrolyzed wood are used to quantify the intrinsic permeability tensor and its evolution with pyrolysis. The results show that pyrolysis only slightly increases porosity, but significantly modifies transport anisotropy: longitudinal and radial permeabilities decrease, while tangential permeability increases markedly, highlighting the major role of evolving constrictions and transverse connectivity. Second, a pore-scale pyrolysis framework developed in PATO, through the integration of rhoPimpleFoam with strong fluidporous coupling and ALE mesh motion, is applied on micro-CT-derived virgin wood geometries to simulate thermochemical decomposition, skeleton shrinkage, gas percolation, and blowing effects. The simulations reproduce the qualitative evolution toward the pyrolyzed structure and illustrate how pore morphology and surrounding flow are altered during decomposition. Together, these results show the potential of OpenFOAM for linking microstructure-resolved characterization and predictive simulation of pyrolyzing wood.

Thermal Management of Electronic Components: Innovations and Modeling

Salmon Fabien, CNRS

The thermal management of electronic components remains an active field with significant potential for improvement. Current solutions primarily rely on fans, which are often noisy, bulky, and inefficient. Phase Change Materials (PCMs) offer a promising alternative for achieving more stable temperature regulation.This work presents three key contributions. First, we propose the use of a gyroid-type porous structure to encapsulate the PCM. This geometry maximizes the exchange surface area with the metallic structure, thereby enhancing heat transfer efficiency.Second, we developed a coupled 3D fluid-structure numerical model that simulates both thermal exchangesincluding conduction and convectionand the mechanical stresses induced by PCM expansion. Built using open-source tools (OpenFOAM, CalculiX, and preCICE), this model enables the prediction of deformation, leakage risks, and thermal contact quality.Finally, our analysis demonstrates that reducing the initial PCM fill ratio is more effective for improving thermal performance than reinforcing the gyroid structure. Additionally, we propose an optimization framework for selecting PCM types and metal materials to further enhance system efficiency.

Validation effort of the porous approach implementation in OpenFoam

Prud'homme Florentin , von Karman Institute

Significant discrepancies have been observed between Openfoam and Ansys Fluent for self-heating porous media. This motivated an investigation of the porous aproach implementation in Openfoam. To reconstruct in Openfoam the Volume-Averaged Navier-Stokes equations (VANS) describing flows in porous media, several utilities need to be combined. The investigation of those utilities revealed inconstencies with the VANS equations. The presentation will show different modifications proposed for the utilities to better reconstruct the VANS equations as well as a term by term validation and a comparison with simple reference cases.

Stochastic Modeling of Hydrodynamic Particle Bridging and Permeability Impairment in Pore Networks

Maya Fogouang Laurez, CNRS - ISTO

Particle transport and retention in porous media are governed by a complex interplaybetween fluid dynamics, particle properties, and pore geometry, leading to inherentlystochastic clogging behaviors. In particular, hydrodynamic particle bridging—wheresuspended particles form stable arches that block pore constrictions—remains poorlycaptured by conventional pore-network models. In this work, we combine high-fidelitynumerical simulations, stochastic modeling, and pore-network upscaling to investigateparticle bridging from the single pore to the network scale. At the scale of a single pore,a coupled CFDDEM approach is employed to analyze particle transport throughconstricted channels, systematically varying constriction angle, particle-to-constrictionsize ratio, flow rate, concentration, and geometric smoothness. The simulationsreveal that clogging is governed by the discrete formation of particle arches,characterized by the average number of particles escaping a constriction prior toblockage. This number decreases with increasing particle concentration and constrictionangle, is weakly dependent on flow rate within the Stokes regime, and exhibits step-wisevariations closely linked to the particle-to-constriction size ratio. Sharper constrictionspromote more frequent and stable bridging events than smoother geometries. Basedon these findings, a stochastic probability law for hydrodynamic bridging is developedand embedded into a probabilistic pore-network model. The model is calibratedusing the CFDDEM results and validated against microfluidic experiments conducted inheterogeneous micromodels representative of porous rock structures. Our frameworksuccessfully reproduces experimental trends in clogging dynamics and permeabilitydecline across a wide range of operating conditions. This multiscale approach extendsthe predictive capability of pore-network models by explicitly accounting forhydrodynamic bridging alongside sieving and aggregation mechanisms.

Simulation of wood drying, pyrolysis and shrinkage for fire resistance applications.

Penicaud Josselin, Université de Bordeaux

The use of wooden structures in construction is increasing worldwide due to their aesthetic qualities and environmental advantages. However, this trend poses significant fire safety challenges that require an improved understanding of their pyrolysis behaviour. A detailed model for simulating wood pyrolysis were written and implemented in the Porous material Analysis toolbox based on OpenFoam. This model extends the pyromechanics model from Lahouze et al. [1]by improving the drying model, which is key to better capturing wood fire dynamics. This includes introducing a mass conservation equation for the liquid phase. Additionally, mechanical properties are expressed as functions of the liquid volume fraction and temperature. This approach allows evaporation to be treated independently from the global pyrolysis progress, leading to a clearer distinction between moisture removal and pyrolysis. The contraction due to evaporation and the one caused by pyrolysis are now modelled as two distinct mechanisms, enabling a description that is more consistent with experimental data. [1]F. Lahouze, W. Jomaa, C. Métayer, M. Meyer, F. Panerai, et J. Lachaud, ń Pyromechanics: A solid mechanics approach to deformation during pyrolysis ż, Fuel, vol. 390, p. 134557, 2025, doi: https://doi.org/10.1016/j.fuel.2025.134557.

Modélisation couplée solide-fluide d'une analyse thermogravimétrique

Trouillet Nell, CEA

Les matériaux composites utilisés comme protection thermique lors de la rentrée atmosphérique sont soumis à des flux thermiques intenses provoquant leur dégradation par pyrolyse. La caractérisation de ce comportement repose notamment sur des essais d'analyse thermogravimétrique (ATG) dont une modélisation numérique a été développée sous PATO. Le modèle adopte une approche multi-régions couplant une région solide, siège de la pyrolyse décrite par une cinétique d'Arrhenius, et une région fluide représentant le gaz inerte environnant. Le couplage thermique à l'interface solide-fluide est pris en compte avec une condition limite de type chtMultiRegion Le rayonnement est simulé avec la méthode fvDOM. Ces travaux ont permis de mettre en évidence et de quantifier un retard de montée en température au coeur des échantillons, avec une différence de température qui peut atteindre 50 K pour les vitesses de chauffe de 100 K/min. Ce travail est critique pour la précision des modèles de pyrolyse développés à partir des caractérisations ATG.

sedExnerFoam: Modeling Sediment Transport and Morphodynamic Evolution

Renaud Matthias, ARTELIA

Scouring, defined as localized erosion induced by flow obstruction around hydraulic structures, is a leading cause of structural failure, particularly for bridges. Despite extensive research, scouring processes remain difficult to predict accurately due to the complex coupling between flow, sediment transport, and bed evolution. This work presents the development of sedExnerFoam, an open-source numerical model designed to simulate sediment transport and morphodynamics within the OpenFOAM framework.The model couples high-resolution hydrodynamics with suspended sediment transport and bed evolution governed by the Exner equation. Bed deformation is dynamically accounted for through mesh motion, allowing two-way interaction between the flow and evolving sediment bed. The model was validated against a series of benchmark cases to ensure numerical accuracy, robustness, and sediment mass conservation.Applications to progressively complex configurations, including dune migration and flow around obstacles, highlight the importance of boundary conditions, flow separation, and grain inertia in morphodynamic predictions. To address limitations of conventional bedload formulations, a bedload saturation approach was introduced, improving sediment redistribution in the presence of flow detachment. Preliminary simulations of scouring around structures demonstrate the models potential for engineering applications, while also identifying key challenges related to mesh quality and sediment transport parameterization that guide future developments.

Modélisation des protections thermiques pyrolysables avec PATO : analyse de la mission Hayabusa

ZAKARIA Nadim, CEA CESTA

La mission Hayabusa a démontré la capacité d'une capsule de retour d'échantillons à survivre à une rentrée atmosphérique à haute vitesse grâce à un bouclier thermique en composite carbone/résine phénolique dense. Ce travail présente la modélisation de la réponse thermique et ablative de cette capsule à l'aide de l'outil open-source PATO (Porous material Analysis Toolbox based on OpenFOAM). En l'absence de données publiques, un modèle matériau représentatif a été reconstruit en combinant les données disponibles dans la littérature avec les propriétés de base du modèle TACOT. Des simulations 1D et 2D axisymétriques ont été réalisées, intégrant un modèle de pyrolyse à trois réactions, une conduction thermique anisotrope et des conditions aux limites aérothermiques dépendantes du temps. Les résultats numériques au point d'arrêt sont comparés à des simulations de référence et à des données d'observation infrarouge en vol. Les simulations 2D montrent un très bon accord avec les observations pour la température de surface. L'influence de l'orientation des fibres de carbone sur la réponse thermique est également étudiée par variation de l'angle de stratification. Des profils de température en profondeur et hors de l'axe d'axisymétrie sont présentés, mettant en évidence les effets multidimensionnels que seule la simulation 2D permet de capturer.

List of Posters

Designing an orifice flow meter operating under laminar regime

Pozzobon Victor, CentraleSupélec

Numerous fields of engineering involve gas delivery to a system. In some cases, this gas supply has to be finely controlled, while in some other cases, an approximate value (ś10%) is sufficient. This is especially the case with bioprocesses, where gas is of secondary interest. Indeed, the process is classically operated in excess of gas (early stages) or at full capacity (late stages). Therefore, an affordable sensor operating in the adequate range and allowing for logging the data would be sufficient for process monitoring. Still, such sensors are challenging to find, especially in the range of interest for laboratory bioprocesses (10 to 1000 Nml/min). The emergence of miniaturized high-performance pressure sensors (1 to 10 000 Pa) allows to envision a new type of orifice flow meters operating under laminar regime. This poster presents a numerical design procedure led with OpenFOAM.

Designing an orifice flow meter operating under laminar regime

Victor Pozzobon[1], Sylvain Salvador[2]

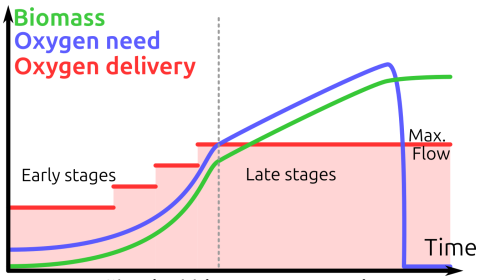
[1] LGPM, CentraleSupélec, Université Paris-Saclay, Centre Européen de Biotechnologie et de Bioéconomie (CEBB), Pomacle, France

[2] IMT Mines Albi-Carmaux, Centre RAPSODEE, UMR CNRS 5302, Campus Jarlard, Albi, Occitanie, FR 81013, France

CONTEXT

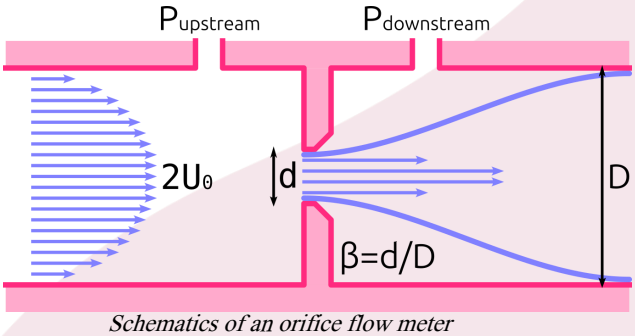
Numerous fields of engineering involve **gas delivery** to a system. In some cases, this gas supply has to be finely controlled, while in some other cases, **an approximate value** (±10%) **is sufficient**. This is especially the case with **bioprocesses,** where gas is of secondary interest. Indeed, the process is classically operated in excess of gas (early stages) or at full capacity (late stages) – Figure on the right. Therefore, an **affordable sensor** operating in the adequate range and **allowing for logging the data** would be sufficient for process monitoring. Still, such sensors are **challenging to find**, especially in the range of interest for laboratory bioprocesses (10 to 1000 Nml/min).

The emergence of miniaturized high-performance pressure sensors (1 to 10 000 Pa) and the now mainstream 3D printing techniques allow to envision microcontroller-embedded for monitoring.



Classical bioprocess operation

SYSTEM & AMBITION



Schematics of an orifice flow meter

An **orifice flow meter** is a monitoring system based on the **pressure drop** across a flow restriction. Several geometries have been engineered over the years (flow nozzle, perforated plates, …)[1]. They are affordable, easy to manufacture, robust **(no moving parts)**, and feature a dimensionless pressure drop coefficient (α in Eq. 1) that does not depend upon Reynolds number in the turbulent regime.

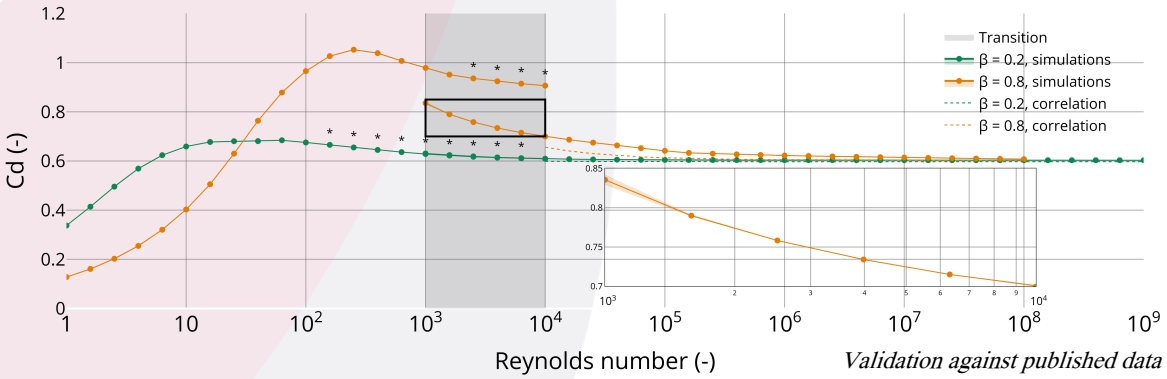
$$\Delta P = \alpha(Re)\,\rho U^2 \qquad (1)$$

Unfortunately, **laboratory flow** (air, 10 to 1000 Nml/min, in 4 mm diameter) falls into the **laminar flow regime**. **OpenFOAM** (*simpleFoam* & *pisoFoam*) is used to **adapt the system** to this regime and **anticipate challenges**.

NUMERICAL TOOL VALIDATION

Domain size and **mesh independence** were guaranteed. **Predictions agree with established literature** (in turbulent regime, RNG k-ε model[2]).

- **2D-axisymmetric** simulations are suited for this system
- **Strong dependence upon β** (d/D) in laminar flow
- **Instabilities** appear for **intermediate Reynolds** numbers[3,4] (* on the graph)



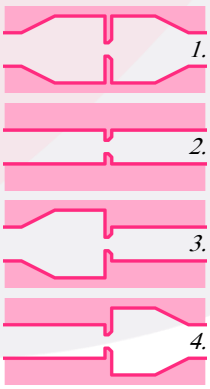
Validation against published data

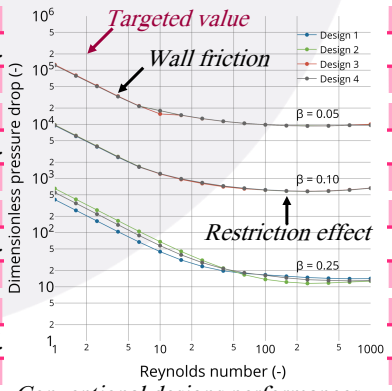
NUMERICAL DESIGN

System response is dominated by the β. Geometrical variations have only a minor effect. In the laminar regime, the pressure drop is the **combination of wall friction** (low Reynolds number) and the **restriction effect** (moderate Reynolds number).

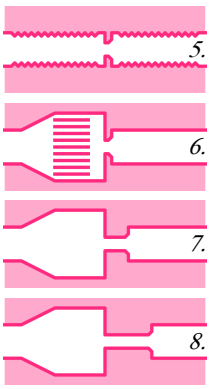
The sensitivity of the system is too low around 10 Nml/min (Re = 2, $\alpha_{min,\,target} = 2\,10^5$).

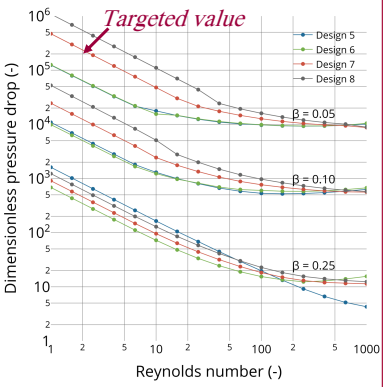
New designs have to be engineered to improve the system response.





Conventional designs performances





Alternative designs performances

1. White, F. M. (1999). Fluid Mechanics. Mcgraw-Hill College.
2. Yakhot, V., Orszag, S. A., Thangam, S., Gatski, T. B., & Speziale, C. G. (1992). Development of turbulence models for shear flows by a double expansion technique. Physics of Fluids A: Fluid Dynamics, 4(7), 1510-1520. https://doi.org/10.1063/1.858424
3. Testud, P., Aurégan, Y., Moussou, P., & Hirschberg, A. (2009). The whistling potentiality of an orifice in a confined flow using an energetic criterion. Journal of Sound and Vibration, 325(4), 769-780. https://doi.org/10.1016/j.jsv.2009.03.046
4. Rees, S. J., & Juniper, M. P. (2010). The effect of confinement on the stability of viscous planar jets and wakes. Journal of Fluid Mechanics, 656, 309-336. https://doi.org/10.1017/S0022112010001060

CONTACT

Victor.Pozzobon@centralesupelec.fr

Simulation numérique couplée des transferts thermo-aérauliques dans la grotte de Lascaux

TARAFT Walid, I2M

La préservation du patrimoine pariétal de la grotte de Lascaux est étroitement liée aucontrôle de son microclimat interne, fortement influencé par les échanges thermiques entre le massif rocheux et lair de la cavité. Dans ce contexte, nous développons une chaîne demodélisation numérique visant à simuler les phénomènes thermo-aérauliques gouvernant lacirculation dair, la conduction thermique et les processus de condensation dans la grotte. La méthodologie repose sur lutilisation conjointe de deux environnements de calculcomplémentaires. Le code CFD NOTUS est mobilisé pour la modélisation tridimensionnellede la conduction dans le massif rocheux et de la convection naturelle de lair dans la cavité. Les transferts de chaleur au sein du massif sont calculés à partir de léquation de la chaleur,permettant dobtenir un champ thermique transitoire réaliste sur lensemble des parois. Cechamp sert ensuite de condition limite pour la simulation de la convection naturelle basée sur les équations de NavierStokes incompressibles sous lapproximation de Boussinesq. Les premiers résultats montrent quune onde thermique issue de la surface se propage dans le massif de manière amortie, avec un retard de phase denviron six mois à dix mètres de profondeur et douze mois à vingt mètres, pour une amplitude denviron 0,6 řC. La simulation de la convection naturelle dans la cavité révèle des gradients thermiques caractéristiques des zones susceptibles de favoriser la condensation. Afin de permettre la modélisation fine des phénomènes de changement de phase à linterface air/paroi, les champs thermiques et aérauliques calculés sous NOTUS sont transférés vers le logiciel OpenFOAM. Ce passage dun code à lautre repose sur une étape dinterpolation des champs physiques, rendue nécessaire par lutilisation de maillages de nature différente : cartésien structuré pourNOTUS et non structuré pour OpenFOAM. Cette procédure dinterfaçage constitue un verrouscientifique essentiel du couplage numérique, garantissant la cohérence physique et laconservation des champs lors du changement denvironnement de calcul, et conditionnant la fiabilité des simulations multiphasiques ultérieures. Les perspectives de ce travail incluent lintégration de méthodes dintelligence artificielle afin daméliorer la prédiction des zones de condensation et doptimiser les temps de calcul, dans lobjectif de contribuer à la préservation durable du microclimat de la grotte de Lascaux.

Simulation numérique couplée des transferts thermo-aérauliques dans la grotte de Lascaux

Walid TARAFT[1], Fabien SALMON[2], Delphine LACANETTE[1], Emmanuelle ABISSET-CHAVANNE[3]*
[1] *Univ. Bordeaux, CNRS, Bordeaux INP, I2M, UMR 5295, F-33400, Talence, France*
[2] *Inria, Univ. Bordeaux, CNRS, Bordeaux INP, IMB, UMR 5251, 200 Avenue de la Vieille Tour, Talence, 33405, France*
[3] *Arts et Métiers Institute of Technology, CNRS, Bordeaux INP, I2M, UMR 5295, F-33400 Talence, France*
* *walid.taraft@u-bordeaux.fr*

Contexte

La grotte de Lascaux, classée au patrimoine mondial de l'UNESCO, contient des peintures pariétales très sensibles aux variations climatiques la stabilité du microclimat dépend de :

- **La conduction thermique dans le massif rocheux**
- **La convection naturelle de l'air**
- **Les phénomènes de condensation et d'évaporation.**

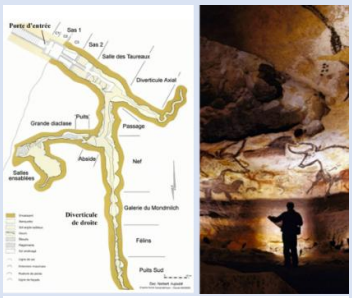


Figure 1: La grotte de Lascaux

Objectifs

Développer une chaîne de simulation numérique capable de reproduire ces phénomènes et d'identifier les zones à risque de condensation.

Deux codes CFD complémentaires sont utilisés :

NOTUS

• conduction thermique dans le massif rocheux

• convection naturelle dans la cavité

OpenFOAM

• modélisation multiphasique

• condensation / évaporation près des parois

Les champs de température et de vitesse calculés avec NOTUS sont exportés puis interpolés sur le maillage OpenFOAM.

Approches numériques

Modèle physique: Conduction thermique dans le massif rocheux.

➢ $\rho C_p \frac{\partial T}{\partial t} = \nabla.(\lambda \nabla T)$

Interprétation physique des termes:

ρ: Densité du matériau $(Kg.m^{-3})$

C_p: Capacité thermique massique $(J.kg^{-1}.K^{-3})$

Terme gauche: accumulation d'énergie thermique dans le matériau.

λ: Conduction thermique $(W.m^{-1}.K^{-1})$

∇T: Gradient de température.

$\nabla.(\lambda \nabla T)$: Diffusion de la chaleur dans le matérieu.

Modèle de convection naturelle dans la Grotte.

➢ $\rho\left(\frac{\partial \vec{V}}{\partial t} + (\vec{V}\cdot\nabla)\vec{V}\right) = -\nabla P + \rho(1-\beta(T-T_0))g + \mu\nabla^2\vec{V}$ (équation de la quantité de movement

➢ $\nabla.\vec{V} = 0$ (équation de la continuité)

➢ $\rho C_p(\frac{\partial T}{\partial t} + \vec{V}\cdot\nabla T) = \nabla\cdot(\lambda\nabla T)$ (équation de lénergie)

Paramètres physiques:

ρ : densité de l'air $(Kg.m^{-3})$

$\vec{V}$: Vecteur de vitesse, P: pression (Pa)

g: accélération de la pesanteur$(m.s^{-2})$, μ: viscosité dynamique

β : Coefficient de dilatation thermique (K^{-1})

Modélisation du changement de phase: evaporation et condensation

➢ $\frac{\partial \alpha_l}{\partial t} + \nabla.(\alpha_l \tilde{U}) = \frac{\dot{m}}{\rho_l}$

➢ $\frac{\partial \alpha_v}{\partial t} + \nabla.(\alpha_v \tilde{U}) = -\frac{\dot{m}}{\rho_v}$

➢ $\nabla.\vec{U} = \left(\frac{1}{\rho_l} - \frac{1}{\rho_v}\right)\dot{m}$

Signefication des variables:

α_l: Fraction volumique du fluide

α_v: Fraction volumique de la vapeur

ρ_l: Densité du liquide

ρ_v: Densité de vapeur

$\dot{m}$: Taux de transfert de masse

Résultats

L'analyse des résultats montre que l'onde thermique issue de la surface est progressivement atténuée et déphasée lors de sa propagation dans le massif. Un retard de phase d'environ 6 mois à 10 m de profondeur et 12 mois à 20 m est observé, avec un écart de température maximal de l'ordre de 0,6 °C. Ce comportement, illustré en Figure 2, met en évidence le phénomène de déphasage thermique, où les températures basses sont progressivement compensées par les températures élevées au fil du temps, traduisant la diffusion amortie de l'onde de chaleur dans le milieu rocheux.

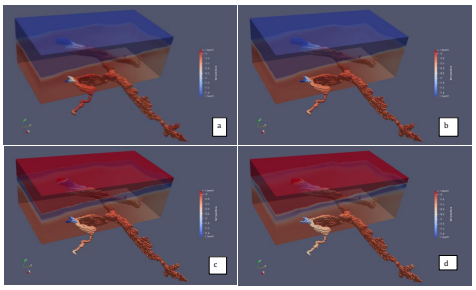


Figure 2: Évolution de la température simulée à travers l'air et le massif rocheux, présentée à des intervalles de 30 jours :(a) 14e mois ;(b) 15e mois ; (c) 16e mois ; (d) 17e mois. Résultats obtenus à l'aide du code NOTUS

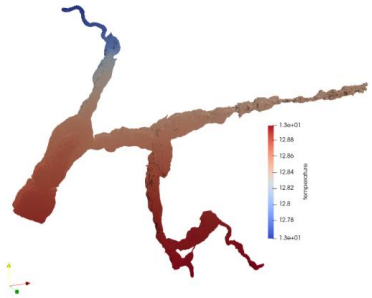


Figure 3: Illustration des conditions initiales et aux limites utilisées dans le modèle numérique.

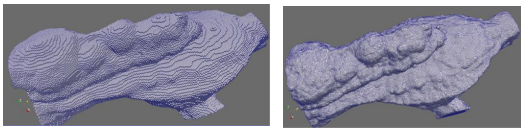


Figure 4: Comparaison entre un maillage structuré (NOTUS, à gauche) et un maillage non structuré (OpenFOAM, à droite) de la Salle des Taureaux, obtenu à l'aide de la commande snappyHexMesh d'OpenFOAM,

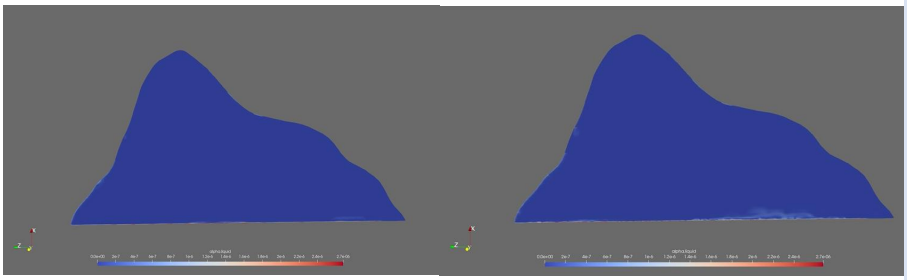


Figure 5: Évolution de la fraction volumique de l'eau dans la grotte de Lascaux au voisinage des parois. L'image à gauche correspond à t=4s et celle à droite à t=7s

Conclusions & Perspectives

Une chaîne de simulation numérique couplée a été développée pour étudier le microclimat de la grotte de Lascaux.

Cette approche permet :

• d'analyser les transferts thermo-aérauliques
• d'identifier les zones favorables à la condensation
• d'améliorer la compréhension du microclimat souterrain.

Perspectives :

- Développer des modèles réduits, capables de reproduire les phénomènes clés avec uncoût de calcul réduit, en vue d'une utilisation rapide pour la prédiction et l'aide à la décision.
- Intégration d'approches d'intelligence artificielle.

Références

DUCASSE, Sylvain et LANGLAIS, Mathieu. Twenty years on, a new date with Lascaux. Reassessing the chronology of the cave's Paleolithic occupations through new 14C AMS dating. *PALEO. Revue d'archéologie préhistorique*, 2019, no 30-1, p. 130-147.

https://notus-cfd.org

F. Salmon, D. Lacanette, H. Lharti, C. Sirieix. Heat transfer in rock masses: Application to the Lascaux Cave (France), International Journal of Heat and Mass Transfer, Elsevier, 207, 124029, 2023.

H. Lharti, F. Salmon, C. Sirieix, J. Riss, D. Lacanette. Caractérisation des propriétés thermiques du massif de Lascaux par méthodes inverses, LHARTI, Habiba, SALMON, Fabien, SIRIEIX, Colette, *et al.*Caractérisation des propriétés thermiques du massif de Lascaux par méthodes inverses. In : *31e Congrès Français de Thermique Thermique et Agroressources*. 2023.

W Dreybrodt, F Gabrovšek, M Perne condensation Corrosion: A Theoretical Approach / Kondenzacijska Korozija: Teoretični Pristop.Acta carsologica, 2005 - ojs.zrc-sazu.si

F. NICOUD, F. DUCROS. Subgrid-Scale Stress Modelling Based on the Square of the Velocity Gradient,Flow, turbulence and Combustion, 1999•Springer

Y. Sun. Description of interCondensatingEvaporatingFoam and implementation of SGS term into volume fraction equation, CFD with OpenSource Software, Chalmers University of Technology, 2022.

https://www.wolfdynamics.com/wiki/meshing_OF_SHM.pdf

Medical sector applications of OpenFOAM

BELLEPERCHE Rodrigue, INGELIANCE TECHNOLOGIES

This poster concerns two studies lead by INGELIANCE :
- Design of a microfluidic mixer
- Diphasic fluid-solid simulation

This poster is confidential.

Simulation de la propagation des feux de forêt ńăzombiesăżă: un problème de combustion en milieux poreux

Dulou Zian, Univ. Bordeaux, CNRS, Bordeaux INP, I2M, UMR 5295, F-33400 Talence, France

La région Nouvelle Aquitaine possède la plus grande surface boisée de France. Le risque de feux de forêt est donc une réelle menace pour ce territoire et sera considérablement aggravé par les effets du réchauffement climatique. Les feux de forêt sont impactés par une spécificité localeă: une partie des sols est composée de matière organique (tourbe, lignite), propice à lapparition des feux zombies (smoldering fire). Un feu zombie est un type de combustion sans flamme qui se propage dans un milieu solide poreux. Il est régi par plusieurs phénomènes couplés : le transport de masse et de chaleur dans le milieu poreux, les réactions de pyrolyse de la matière organique, les réactions d'oxydation impliquant la diffusion de l'oxygène au sein du milieu poreux. Pour simuler ce phénomène, le code de calcul PATO basé sur OpenFOAM et Mutation++ est utilisé. Il permet de simuler les transferts de chaleur et de masse dans le solide ainsi que les réactions de pyrolyse et doxydation afin de suivre la dynamique des feux zombies. Le code permettra de déterminer les paramètres conditionnant le démarrage, la propagation et lextinction des feux ainsi que les flux de chaleur apportés en surface

Compréhension des feux de forêt zombie : application aux méga-feux de Nouvelle-Aquitaine

Zian Dulou[1,2], Cécile Gaborieau[1,2], Franck Richard[3], Jean Lachaud[1,2]

[1] Univ. Bordeaux, CNRS, I2M, UMR 5295, F-33400, Talence, France
[2] Arts et Métiers Institute of Technology, CNRS, I2M, UMR 5295, F-33400 Talence, France
[3] Univ. Poitiers, CNRS, ISAE-ENSMA, Institut Pprime, UPR 3346, F-86360 Chasseneuil-du-Poitou, France

Contexte

Un feu zombie (smoldering fire) est un type de combustion sans flamme qui va se propager dans un milieu solide poreux riche en matière organique (tourbe, lignite). A la différence des feux de forêt, les feux zombies se caractérisent par une propagation lente (cm/h) et des températures relativement faibles (500-600°C). Ces feux se propagent en profondeur pendant des semaines ou des mois et peuvent déclencher des feux de surface. Les feux zombies sont à l'origine de la reprise du feu de Landiras en 2022.

Les objectifs sont de :
- Caractériser les sols inflammables de la région de Landiras
- Simuler les conditions d'ignition et d'extinction
- Simuler la propagation des feux zombies

Le code de calcul PATO (Porous material Analysis Toolbox based on OpenFOAM) est utilisé pour simuler les transferts de chaleur et de masse dans les milieux réactionnels poreux.



[Rein 2008]

Equations

Conservation de la masse

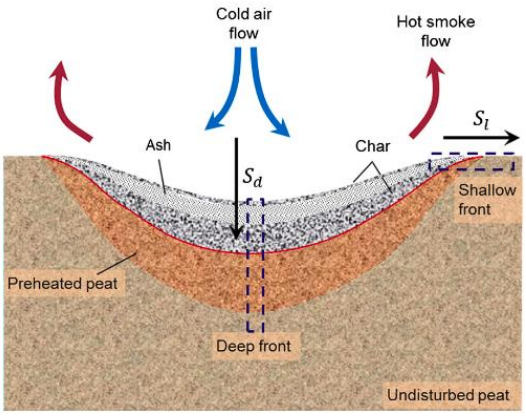
$$\partial_t \left(\varepsilon_i \langle \rho_i \rangle^i\right) + \nabla \cdot \left(\varepsilon_i \langle \rho_i \rangle^i \langle \mathbf{v_i} \rangle^i\right) = \mathcal{M}_i \langle \omega_i \rangle$$

Conservation de la quantité de mouvement (Loi de Darcy)

$$\langle \mathbf{v}_g \rangle^g = -\frac{1}{\varepsilon_g \langle \mu \rangle^g} \underline{\underline{\mathbf{K}}} \cdot \nabla \langle p \rangle^g$$

Conservation de l'énergie

$$\sum_{i\in\{s,l,g\}} \varepsilon_i \langle \rho_i \rangle^i \langle c_{p,i} \rangle^i \partial_t \langle T \rangle - \sum_{i\in\{s,l,g\}} \nabla \cdot (\mathbf{k}^{\text{app}} \cdot \nabla \langle T \rangle) = \left| \begin{array}{l} - \sum_{j\in\{[1,N_s],l\}} h_j(T)\, \partial_t \left(\varepsilon_s \langle \rho_j \rangle^j\right) - \sum_{j\in N_g} \nabla \cdot \left\langle \mathbf{Q}_j^d \right\rangle + q^r \\ - \sum_{j\in[1,N_g]} \left[h_j(\langle T \rangle)\, \partial_t \left(\varepsilon_g \langle \rho_g \rangle^g \langle y_j \rangle^g\right)\right] + \partial_t \left(\varepsilon_s \langle p_g \rangle^g\right) + \varepsilon_g \langle \mathbf{v}_g \rangle^g \cdot \nabla \langle p_g \rangle^g \\ - \sum_{i\in\{s,l,g\}} \nabla \cdot \left(\varepsilon_i \langle \rho_i \rangle^i \langle h_i \rangle^i \langle \mathbf{v}_i \rangle^i\right) \end{array} \right.$$



[Huang 2014]

Réactions chimiques

On considère un schéma à 5 réactions chimiques avec 5 espèces solides dont 2 chars différents :

Séchage

Tourbe(H_2O) → Tourbe + H_2O

Pyrolyse

Tourbe → α-Char + Gas

} Endothermique

Oxydation

Tourbe + O_2 → β-Char + Gas
β-Char + O_2 → Cendre + Gas
α-Char + O_2 → Cendre + Gas

} Exothermique

La propagation des feux zombies repose sur l'équilibre entre les réactions endothermiques (en bleu) et les réactions d'oxydation exothermiques (en vert). Les feux zombies sont donc limités par l'accès en oxygène qui alimente les réactions d'oxydations. Ils sont un mécanisme complexe entre réaction endo/exo thermiques, diffusion de l'oxygène et perte de chaleur.

Les réactions sont simulées par des lois d'Arrhenius :

$$k_r = A_r \langle T \rangle^{n_r} \exp\left(-\frac{E_r}{R\langle T \rangle}\right)$$

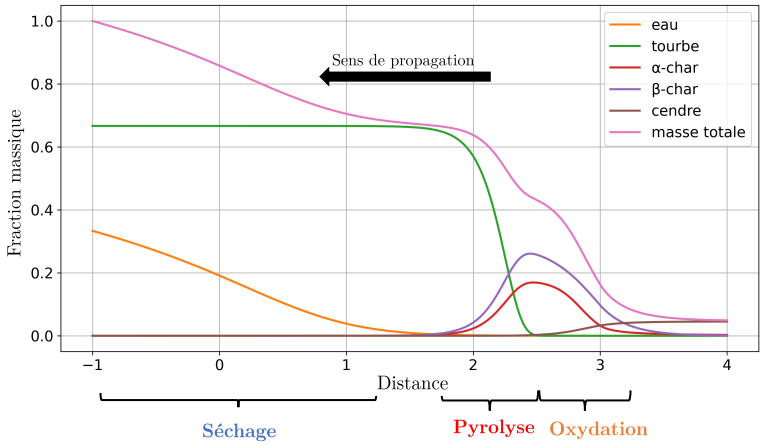
Le taux de production d'une espèce solide s'écrit donc :

$$\langle \omega_i \rangle = \sum_{r=1}^{N_r} \left[\nu_{i,r} k_r \langle X_{i,r} \rangle^{m_{i,r}} \langle X_{O2} \rangle^{m_{O2,r}}\right]$$

Avec :
- k_r l'avancement de la réaction r
- $\nu_{i,r}$ le coefficient stoechiométrique
- $\langle X_i \rangle$ la concentration molaire de l'espèce i
- $m_{i,r}$ l'ordre de la réaction
- A_r, E_r et n_r les coefficients d'Arrhenius

Résultats

En résolvant seulement la conservation de la masse avec un profil de température imposé, la structure du front de réaction est déterminée par différences finies avec un code python [Huang 2014]. Ceci illustre les mécanismes réactionnels des feux zombies. On constate 3 zones : la zone de séchage, la zone de pyrolyse et la zone d'oxydation des chars. Ce modèle permet de prédire les concentrations des espèces solides présentes à partir des coefficients d'Arrhenius.



Références

Huang, Xinyan et Guillermo Rein (2017). "Downward spread of smouldering peat fire : the role of moisture, density and oxygen supply". In : International Journal of Wildland Fire 26.11, p. 907-918.

Rein, Guillermo et al. (2008). "The severity of smouldering peat fires and damage to the forest soil". In : CATENA 74.3, p. 304-309.

Huang, Xinyan et Guillermo Rein (juin 2014). "Smouldering combustion of peat in wildfires : Inverse modelling of the drying and the thermal and oxidative decomposition kinetics". In : Combustion and Flame 161.

Ignition and propagation of a combustion reaction front in peat

Romero-Menco Fredys de Jesus, Doctoral Student

The Nouvelle-Aquitaine region faces a high wildfire risk, exacerbated by zombie fires smouldering underground fires in peat and lignite soils that can reignite surface blazes, as seen in Landiras (2022) - . As part of the GRIFON project, this work investigates such fires through combined experimental and numerical approaches. These fires are governed by coupled heat and mass transport, pyrolysis, and heterogeneous oxidation reactions (smouldering) in porous media. To date, kinetic characterization of the pyrolysis process has been performed using thermogravimetric analysis under inert atmospheres. Pyrolysis parameters were extracted using evolutionary optimization algorithms (GA) in order to know the behavior of the fuel at different conditions. These kinetic parameters will serve as inputs for a multiscale (micro, meso, macro) numerical model to be implemented in PATO, a porous media toolbox based on OpenFOAM. The model aims to simulate the propagation of the underground smouldering front, with future extensions including two-temperature gassolid coupling and surface vegetation ignition via FireFOAM.

Ignition and Spread of a Smouldering Front in Porous Media: *Application to Zombie Fires Issue*

ROMERO-MENCO, FREDYS[1]; RICHARD, frank[1]; ROGAUME, thomas[1]
[1] Departement of Fluides, Thermique, Combustion, Institut P', UPR 3346 CNRS, Université de Poitiers, ISAE-ENSMA, CEDEX 9, 86073 Poitiers, France

1. Introduction

Wildfires are a major threat to biodiversity and forest ecosystems. Smoldering combustion is a flameless heterogeneous combustion characterized by low temperatures (450–750°C), slow propagation velocities (3.3×10^{-4} – 1.62×10^{-2} m/min), and absence of visible flames. It is the ***most persistent*** form of combustion and comprises four subfronts: preheating, drying, pyrolysis, and oxidation.

Peat is an organic-rich porous medium (cellulose ~40%, hemicellulose ~21%, lignin ~24%; HHV ~20 MJ/kg) prone to smoldering. Smoldering fronts in peat propagate through in-depth (forward) and lateral spread, potentially persisting for years undetected under soil, making them extremely difficult to suppress.

The mechanisms controlling ignition and spread under local peat composition and climate remain poorly understood.

2. Motivation

The 2022 Gironde wildfires illustrated the extreme hazard of peat smoldering. A front formed undetected in the peat layer, underwent transition to flaming combustion, and the associated smoke plumes persisted for more than two and a half years after the main event — a paradigmatic case of the 'zombie fire' phenomenon.

34000 ha consumed by flaming fire	**7400** ha additional area from smoldering	**2,5+** years smoke plumes persisted

2. Objectives

General

Experimentally and numerically characterize the ignition, propagation, and transition to flaming of smoldering fronts in peat under conditions representative of Nouvelle-Aquitaine.

Specifics

•Characterize spread rate and thermal structure as a function of peat physical properties (porosity, density, thermal conductivity).

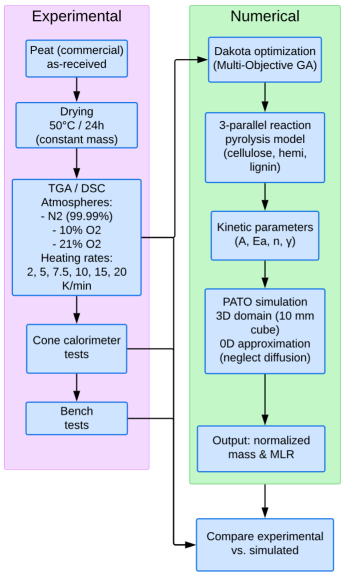
•Determine the effect of environmental conditions on ignition thresholds of smoldering fronts in peat.

•Identify critical conditions governing the transition from smoldering to flaming combustion.

•Implement heterogeneous smoldering reactions in PATO using a two-temperature model for gas–solid heat exchange.

•Couple the PATO smoldering model with fireFoam to simulate gas-phase combustion and the smoldering-to-flaming transition.

3. Methodology



On the moment a first approximation with pyrolysis process has been realized

4. Key Results

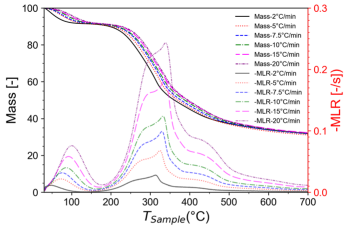


Figure 1. *Thermogravimetric analysis of peat under non-oxidative atmosphere (N_2)*

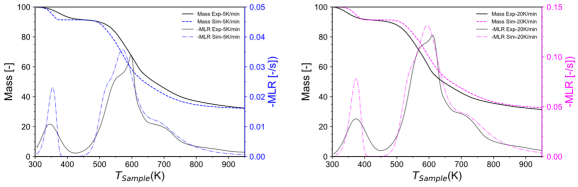


Figure 2. *Comparison between experimental TGA and DSC and numerical simulation results.* ***Left:*** *HR 5K/min.* ***Right:*** *HR 20K/min.*

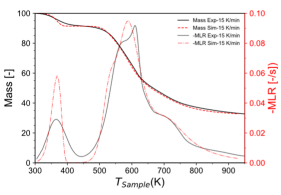


Figure 3. *Comparison between experimental TGA and DSC and numerical blind simulation results at HR of 15K/min.*



Figure 4. *Peat in borosilicate beaker in cone calorimeter test. Highligthed in red it can be seen the smoldering front formation.*

5. Discusion

The results under non-oxidative atmosphere shows that around 34% of peat corresponds to mix between carbon and ashes. Moreover it could be appreciate three main peaks during the pyrolysis process between 200 and 500°C. There is a good agreement between experimental and numerical results.

The highest deviation it is observed in the drying process which was not included in the optimization process. This suggest that despite the fact that drying it is not a chemical process should be considered in the optimization as some authors recommends. In general, the peaks are reproduced by simulation adequately. The most significative difference can be observed in the results for a HR of 5°C/min.

6. Conclusions

Three main pyrolysis peaks (550, 625, 700 K) were identified, with ~34 % char+ash residue. The three parallel reaction model successfully predicts mass loss for 5, 15 and 20 K/min under N_2. Largest deviation at low heating rate (5 K/min, $\Delta T \approx 50$ K) could be due to exclusion of drying; inclusion of a drying sub model is recommended.

7. References

- Ohlemiller, T. J. (1985). Modeling of smoldering combustion propagation. Progress in energy and combustion science, 11(4), 277-310.
- Huang, X., & Rein, G. (2014). Smouldering combustion of peat in wildfires: Inverse modelling of the drying and the thermal and oxidative decomposition kinetics. Combustion and Flame, 161(6), 1633-1644.
- Leroy-Cancellieri, V., Cancellieri, D., Leoni, E., Simeoni, A., & Filkov, A. I. (2014). Energetic potential and kinetic behavior of peats. Journal of Thermal Analysis and Calorimetry, 117(3), 1497-1508.
- Cuong Dinh, D., Richard, F., Batiot, B., & Rogaume, T. (2024, November). A Comprehensive Model for Wood Pyrolysis Incorporating Detailed Chemical Reactions and Porous Medium Interactions. In Journal of Physics: Conference Series (Vol. 2885, No. 1, p. 012012). IOP Publishing.

Acknowledgments

This work is part of the GRIFON project funded by the Nouvelle-Aquitaine Region (France). The authors gratefully acknowledge the financial support provided. Special thanks to Ms. Marc Poisson for their assistance in the experimental tests; and to Dr. Rogaume, and Dr. Richards for their continuous guidance…and patience !

*Corresponding author: fredys.romero.menco@univ-poitiers.fr

Modélisation numérique de la pyrolyse de bois sous OpenFOAM : prédiction de la spéciation des gaz par schémas cinétiques détaillés

D'ANTONI Joanna, I2M (Institut d'Ingénierie et de Mécanique)

La modélisation de la pyrolyse de la biomasse nécessite de coupler les transferts multiphysiques en milieu poreux à une chimie complexe. Ce travail présente limplémentation d'un solveur intégrant des mécanismes cinétiques compétitifs au sein de la boîte à outils PATO (Porous material Analysis Toolbox based on OpenFOAM) afin de simuler la conversion thermochimique de solides réactifs.L'originalité de l'approche réside dans l'utilisation des schémas semi-détaillés du groupe CRECK. Ce modèle s'affranchit des cinétiques globales limitées tout en restant numériquement plus efficient que les mécanismes fondamentaux grâce à une approche par regroupement d'espèces (lumping). Appliquée à un pellet de bois de pin maritime, la simulation couple conduction thermique, transport des gaz, déformation du solide et cinétique chimique. Lobjectif est de caractériser finement la spéciation des gaz (H2, CO, CH4, goudrons) et la nature du char produit afin d'en évaluer la réactivité pour des procédés de gazéification.Les résultats démontrent la capacité du solveur à prédire les rendements et la qualité des produits en fonction des conditions opératoires de pyrolyse. Limplémentation de cette brique logicielle supplémentaire permet denrichir les capacités prédictives d'OpenFOAM, constituant ainsi un outil daide à la décision pour le génie des procédés et l'optimisation des vecteurs énergétiques bio-sourcés.

Numerical modeling of wood pyrolysis on OpenFOAM: prediction of gas speciation through detailed kinetic schemes

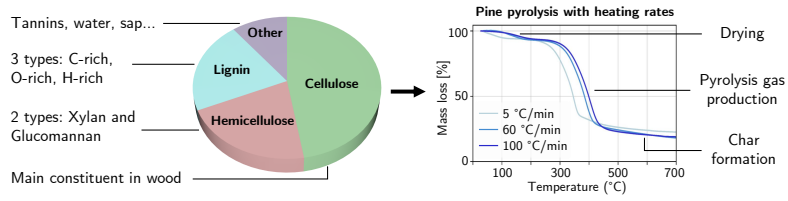
Joanna D'Antoni[1,2], Amine Ben Abdelwahed[1,2], Wahbi Jomaa[1,2], Jean Lachaud[1,2]

[1] *Univ. Bordeaux, CNRS, Bordeaux INP, I2M, UMR 5295, F-33400, Talence, France*

[2] *Arts et Métiers Institute of Technology, CNRS, Bordeaux INP, I2M, UMR 5295, F-33400 Talence, France*

Context

Wood pyrolysis: Thermal degradation of wood without oxygen. Can be used for energetic purposes, or to produce molecules of interest. Decomposition and products quantities depend on the composition and heating conditions:



PATO: (Porous material Analysis Toolbox based on OpenFOAM) [1] Models pyrolysis with parallel and simplified reactions. Does not capture the competitive nature of the reactions. Does not allow gas fraction prediction.

Objectives: Implement competitive mechanisms from literature, building on previous work [2], and adapt them to experimental data for cellulose, xylan, lignin, and pine at different heating rates.

Strategy: Ranzi's mechanism from 2017 [3] with the improvements added on cellulose [4]. Calibration and modification of the original mechanism to better fit the experimental results. Simulations of a small particle in TGA oven (set heating rate, homogeneous temperature).

Conservation equations

Mass conservation equations: [1,2,5]

$$\frac{\partial \epsilon_{s,i}\langle\rho_{s,i}\rangle^i}{\partial t} + \nabla\cdot(\epsilon_{s,i}\langle\rho_{s,i}\rangle^i\langle\boldsymbol{v_s}\rangle^s) = \sum_{i\in N_s} M_i\langle\pi_i\rangle \quad \text{Solid phase}$$

$$\frac{\partial \epsilon_g\langle\rho_g\rangle^g}{\partial t} + \nabla\cdot(\epsilon_g\langle\rho_g\rangle^g\langle\boldsymbol{v_g}\rangle^g) = -\sum_{i\in N_s} M_i\langle\pi_i\rangle \quad \text{Gas phase}$$

Accumulation — Transport — Rate of mass loss/prod

Momentum conservation equations:

$$\nabla\cdot\langle\underline{\underline{\sigma}}\rangle^s = \mathbf{0} \quad \text{Solid phase}$$

$$\langle\boldsymbol{v_g}\rangle^g - \langle\boldsymbol{v_s}\rangle^s = \frac{-1}{\epsilon_g\langle\mu_g\rangle^g}\,\underline{\underline{K}}\cdot\nabla\langle p_g\rangle^g \quad \text{Gas phase}$$

Permeability

Energy conservation equation:

$$\frac{\partial\left(\langle\rho_t\rangle\langle e_t\rangle\right)}{\partial t} + \nabla\cdot(\epsilon_g\langle\rho_g\rangle^g\langle h_g\rangle^g\langle\boldsymbol{v_g}\rangle^g) = \nabla\cdot\left(\langle\underline{\underline{k}}\rangle\cdot\nabla\langle T\rangle\right) - \nabla\cdot\left(\sum_{i\in N_s}\epsilon_{s,i}\langle\rho_{s,i}\rangle^i\langle h_{s,i}\rangle^i\langle\boldsymbol{v_s}\rangle^s\right)$$

Accumulation — Gas transport — Conduction — Solid transport

Chemical reaction modeling

Chemical kinetic equations:

The general form of a chemical mechanism composed of N_s species S_i and N_r reactions:

$$\sum_{i\in N_s}\nu^f_{i,r}S_i \underset{k^b_r}{\overset{k^f_r}{\rightleftharpoons}} \sum_{i\in N_s}\nu^b_{i,r}S_i \quad \forall r\in N_r$$

The total mass production rate for a species i due to all reactions considered is given by:

$$\langle\pi_i\rangle = \sum_{r\in N_r}\left[(\nu^f_{i,r}-\nu^b_{i,r})\left(k^f_r\prod_{i\in N_s}\langle X_i\rangle^{m^f_{i,r}} - k^b_r\prod_{i\in N_s}\langle X_i\rangle^{m^b_{i,r}}\right)\right]$$

Mass prod/loss rate

With the Arrhenius law:

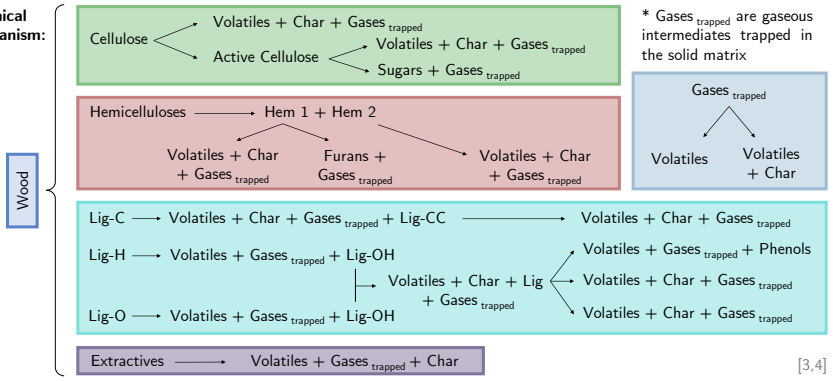
$$k^f_r = \mathcal{A}_r\langle T\rangle^n\exp\left(\frac{-\mathcal{E}_r}{R\langle T\rangle}\right)$$

With the species molar fraction:

$$\begin{cases}\langle X_i\rangle = \varepsilon_i\,\langle\rho_i\rangle^i/M_i\\ \langle X_i\rangle = \langle\rho_g\rangle^g\,\langle y_i\rangle^g/M_i\end{cases}$$

[1,2,5]

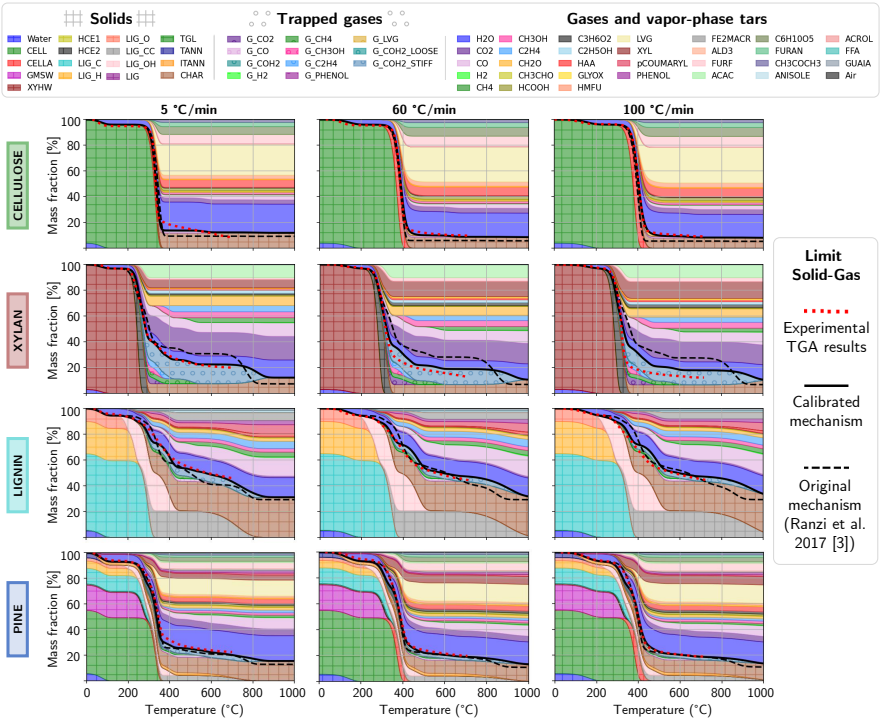
Chemical mechanism: [3,4]



Results

The following graphs show the evolution of mass fractions during pyrolysis for different wood components at three heating rates. The initial solid fraction (hatched) decreases with temperature as new species are formed: intermediate solids, trapped gases (solid markers) that are subsequently released from the solid matrix, and finally gases and non-condensed tars (solid colors).

NB: Although pine hemicellulose is mainly composed of glucomannans, xylan was used as a model compound because no suitably pure glucomannan was commercially available.



Implementation of competitive mechanism allows tracking the evolution of 50+ species during pyrolysis, showing heating rate effects on product distribution. Calibration and adaptation of the original mechanism improve the prediction of solid evolution.

Can you spot it? The original mechanism parameters have been chosen to better represent wood pyrolysis, whereas this work has been calibrated on the individual components !

Conclusions & Perspectives

New developments:

- Competitive mechanisms were successfully implemented and validated against benchmark software in 0D configurations to verify the chemistry.
- The energy equation was validated in a 0D test case against an analytical solution.
- 1D and 2D-axisymmetric simulations can now be coupled with the solid deformation solver recently developed [5]. Simulation times range from a few seconds to a few minutes.
- The mechanism was adapted to improve agreement with experimental solid residue evolution as a function of temperature.
- The Arrhenius parameters (E, A, and n) were chosen to remain consistent with values reported in the literature and in a previous study [6].

The next steps:

- The mechanism could still be improved to better reproduce experimental gas production and species evolution.
- Interactions between biomass components may delay their decomposition; additional reactions could be introduced to account for this phenomenon.

References

[1] J. Lachaud, J. B. Scoggins, T. E. Magin, M. G. Meyer, and N. N. Mansour, "A generic local thermal equilibrium model for porous reactive materials submitted to high temperatures," *International Journal of Heat and Mass Transfer*, vol. 108, part B, pp. 1407–1418, 2017. doi:10.1016/j.ijheatmasstransfer.2016.11.067.

[2] J. Chevalier, *Modélisation des transferts thermiques dans les matériaux composites pyrolysables*, PhD thesis, Université de Bordeaux, 2024. doi:10.70675/2c970b6a8c78z4c69z8e67zbb2d9ced0b60.

[3] E. Ranzi, P. E. A. Debiagi, and A. Frassoldati, "Mathematical modeling of fast biomass pyrolysis and bio-oil formation. Note I: Kinetic mechanism of biomass pyrolysis," *ACS Sustainable Chemistry & Engineering*, vol. 5, no. 4, pp. 2867–2881, 2017. doi:10.1021/acssuschemeng.6b03096.

[4] P. Debiagi, V. Piazza, M. Papagni, A. Beretta, A. Frassoldati, and T. Faravelli, "Cellulose pyrolysis kinetic model: Detailed description of volatile species," *Proceedings of the Combustion Institute*, vol. 40, no. 1–4, p. 105651, 2024. doi:10.1016/j.proci.2024.105651.

[5] F. Lahouze, W. Jomaa, C. Métayer, M. Meyer, F. Panerai, and J. Lachaud, "Pyromechanics: A solid mechanics approach to deformation during pyrolysis," *Fuel*, vol. 390, 2025. doi:10.1016/j.fuel.2025.134557.

[6] J. D'Antoni, A. Ben-Abdelwahed, C. Gaborieau, A. Duphil, W. Jomaa, et al., "Biomass pyrolysis: Thermodynamic parameters review and determination through TGA," *Proceedings of the 37th Int. Conf. on Efficiency, Cost, Optimization, Simulation and Environmental Impact of Energy Systems (ECOS 2024)*, Rhodes, Greece, Jun. 2024, pp. 2042–2053. doi:10.52202/077185-0175.

Mixt3SedFOAM: Improved Sediment Transport Prediction via Wall-Free Low-Re Turbulence Modeling

Raesi Ramin, KU Leuven

Mixt3SedFOAM is a physics-based sediment transport model for simulating free-surface flows, developed and implemented in OpenFOAM. The model is based on multiphase mixture theory to describe interactions between water and sediment and employs the VOF method for free-surface tracking. Interphase momentum transfer is modeled through an additional slip velocity closure that accounts for drag, turbulent dispersion, and shear-induced diffusion. Accurate prediction of sediment transport also requires resolving the inner boundary layer, where bedload transport occurs. To address this, a new wall-free low-Reynolds-number k turbulence model has been developed, with damping functions formulated in terms of the non-dimensional turbulent eddy viscosity normalized by the effective viscosity. The model has been systematically validated against benchmark cases using OpenFOAM, including turbulent channel flow, flow over a backward-facing step, and flow over a periodic hill. The results show good agreement with available DNS and experimental data, demonstrating the models ability to capture turbulence characteristics under both favorable and adverse pressure gradients. Subsequently, the newly developed turbulence model has been incorporated into Mixt3SedFOAM. Its performance has been assessed and validated against experimental data for sediment-laden flows in both dilute and non-dilute regimes, where, in the latter case, particleparticle interactions cannot be neglected.

KU LEUVEN

Department of Civil Engineering

mixt3SedFOAM: improved sediment transport prediction via wall-free Low-Re turbulence modeling

Ramin Raesi[1], Erik A Toorman[1]

[1]Hydraulics and Geotechnics, Department of Civil Engineering, KU Leuven, 3001 Leuven, Belgium

Abstract

Accurate sediment transport modeling requires high-fidelity numerical tools capable of capturing both large- and small-scale flow phenomena. Mixt3SedFOAM, developed by Ouda and Toorman [1], is a three-phase mixture-theory-based solver for sediment transport in free-surface flows. In this framework, interphase momentum transfer is modeled through a slip-velocity closure accounting for drag force, turbulent dispersion, and shear-induced diffusion. However, the original turbulence modeling approach relies on wall functions, which limits the accurate prediction of bed-load transport and bed shear stress. Moreover, the presence of a sediment bed with varying height restricts the applicability of conventional wall-dependent low-Reynolds-number (LRN) turbulence models.

Recently, a new wall-free LRN *k-ε* model was developed by Raesi and Toorman [2], employing damping functions based on the dimensionless eddy viscosity normalized by the effective viscosity. The developed model was validated for several turbulent benchmark flows, including channel flow, backward-facing step flow, and flow over a periodic hill. Comparisons with available DNS and experimental data demonstrated that the proposed model effectively captures the flow dynamics and turbulence quantities across these cases. Therefore, in the present study, this LRN model is integrated into Mixt3SedFOAM to accurately resolve the inner boundary layer and improve sediment transport predictions. Channel flows with both low and high sediment concentrations are selected for model validation. In summary, the combination of a wall-free LRN *k-ε* model and appropriate additional dissipation mechanisms due to the presence of sediments is essential for accurately predicting sediment-laden channel flows.



Governing Equations

➤Sediment Mass Balance Eq: $\frac{\partial \alpha_s}{\partial t} + \nabla \cdot (\alpha_s v) + \nabla \cdot \left[\alpha_s \left(\frac{\alpha_w}{\gamma} - \frac{\alpha_s \alpha_w (\rho_s - \rho_w)}{\rho} + \frac{\alpha_s \alpha_w \alpha_a (1-S)}{\gamma(\alpha_s S + \alpha_w)} \right) w \right] = 0$

➤Fluid Mass Balance Eq: $\frac{\partial \alpha_w}{\partial t} + \nabla \cdot (\alpha_w v) + \nabla \cdot \left[\alpha_w \left(-\frac{\alpha_s}{\gamma} - \frac{\alpha_s \alpha_w (\rho_s - \rho_w)}{\rho} + \frac{\alpha_s \alpha_w \alpha_a (1-S)}{\gamma(\alpha_s S + \alpha_w)} \right) w \right] + \nabla \cdot (\alpha_w \alpha_a U_c) = 0$

➤3-phase Momentum Conservation Eq: $\frac{\partial \rho v}{\partial t} + \nabla \cdot (\rho v v) = -\nabla (p_{rgh} + p_s) + \nabla \cdot [\bar{\tau} + \tau^T + \tau^D_{s-w} + \tau^D_{m-a}] - gh\nabla(\rho) + 2\sigma H \nabla(\gamma)$

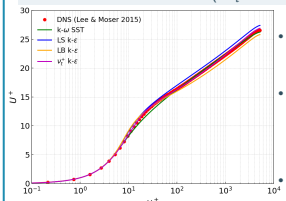
➤LRN mixture *k-ε* model:

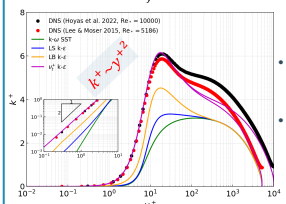
$\frac{\partial \rho k}{\partial t} + \nabla \cdot (\rho v k) = \nabla \cdot \left[\left(\mu_m + \frac{\mu_t}{\sigma_k} \right) \nabla k \right] + 2\mu_m D : D - \rho\varepsilon - G_k - D_k$

$\frac{\partial \rho \varepsilon}{\partial t} + \nabla \cdot (\rho v \varepsilon) = \nabla \cdot \left[\left(\mu_m + \frac{\mu_t}{\sigma_\varepsilon} \right) \nabla \varepsilon \right] + f_1 C_{1\varepsilon} \frac{\varepsilon}{k} 2\mu_m D : D - f_2 C_{2\varepsilon} \rho \frac{\varepsilon^2}{k} - G_\varepsilon - D_\varepsilon$

Clear-Water Flow

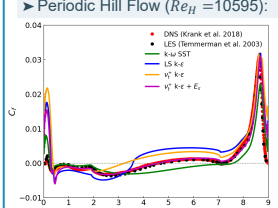
➤Turbulent Channel Flow ($Re_\tau = 5186$):

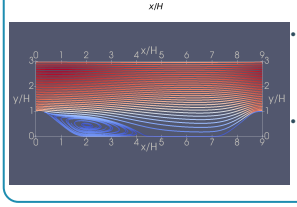




- Accurate mean velocity prediction.
- Good agreement with DNS data of turbulence parameters.
- Correct near-wall asymptotic behavior achieved without wall-distance dependence.
- Stable wall-free low-Re turbulence modeling.
- Inner boundary layer resolved directly with $y^+ < 1$

➤Periodic Hill Flow (Re_H =10595):





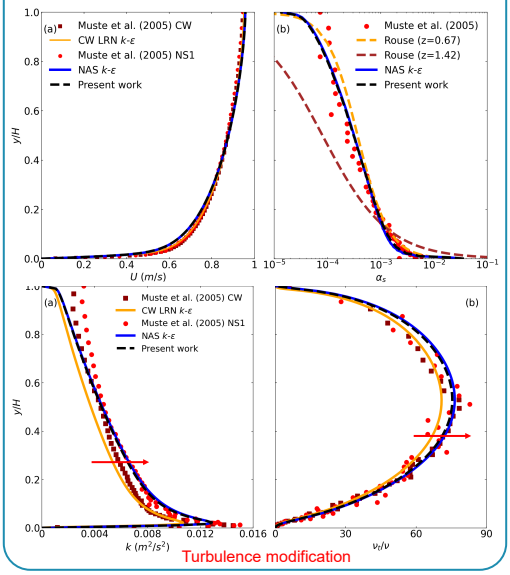
- Accurate prediction of separation and reattachment regions.
- Good agreement with reference C_f profiles.
- Captures recirculation bubble and shear-layer development.
- Enhanced prediction of separated shear-layer recovery using E_ε
- Demonstrates robustness of the model for complex separated turbulent flows.

✓ Accurate prediction of both equilibrium and separated turbulent flows

Low Concentration Sediment Flow

➤Dilute sediment-laden flow (Muste et al. (2005)):

- Accurate prediction of the flow field using the wall-free LRN mixture *k-ε* model.
- Steeper velocity gradients in dilute sediment-laden flow.
- "Enhanced turbulence levels even at low sediment concentrations.
- Flow modifications are primarily governed by altered velocity gradients rather than additional sediment dissipation terms.



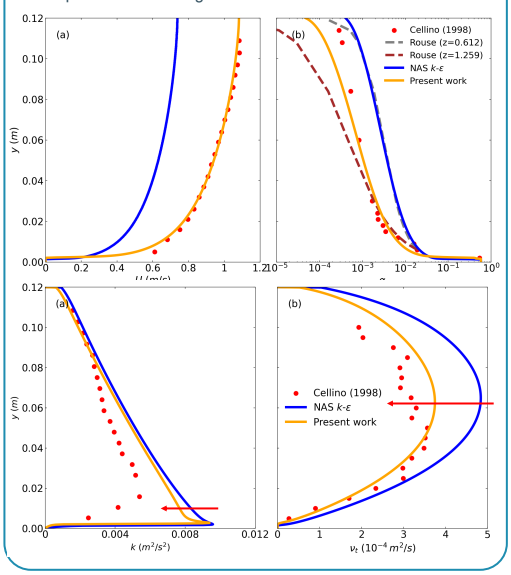
Turbulence modification

✓ Even dilute sediment concentrations modify near-wall turbulence

High Concentration Sediment Flow

➤Non-Dilute sediment-laden flow (Cellino (1998) Q70S025):

- Accurate prediction of dense sediment-laden flow behavior using the wall-free LRN mixture *k-ε* model.
- Strong sediment stratification significantly modifies turbulence structure.
- Improved prediction of flow behavior compared with the standard NAS *k-ε* model.
- Turbulence modulation becomes dominated by sediment-induced dissipation effects at high concentrations.



✓ Dense sediment concentrations strongly alter flow structure

References

[1] Ouda, M., Toorman, E.A., 2019. Development of a new multiphase sediment transport model for free surface flows. International Journal of Multiphase Flow 117, 81–102.
[2] Raesi, R., Toorman, E.A., 2026. Development and assessment of a new wall-free low-Reynolds-number k–ε turbulence model. International Journal of Heat and Fluid Flow 950120, 110382.
[3] Cellino, M., 1998. Experimental study of suspension flow in open channels. Ph.D. thesis. EPFL.854.
[4] Muste, M., Yu, K., Fujita, I., Ettema, R., 2005. Two-phase versus mixed-flow perspective on suspended sediment transport in turbulent channel flows. Water resources research 41

❑ The wall-free Low-Re turbulence framework enables accurate prediction of turbulence modulation from clear-water to dense sediment-laden transport flows.

Research Foundation Flanders
Opening new horizons

9th French/Belgian OpenFOAM Conference

Ramin Raesi

Développement de benchmarks pour la validation des modèles pyromécaniques pour la communauté pyrolyse

Bideau Gloire, Institut de Mécanique et d'Ingénierie (I2M)

Ce travail porte sur le développement dun cas-test dablation (Ablation Test-case 4.0), qui est une extension dun cas de référence existant (Ablation Test-case 1.0) intégrant désormais des effets pyromécaniques. Le cas de référence est un problème unidimensionnel, ce qui nous permet de nous concentrer uniquement sur les phénomènes internes. Létude considère un échantillon de 5 centimètres d'épaisseur de matériau ablatif isotrope de type TACOT.Initialement, le matériau est à température ambiante (298 K) et à pression atmosphérique. Une condition thermique est appliquée à sa surface supérieure: la température monte rapidement jusqu'à environ 1644 K en 0,1 seconde, puis reste constante pendant une minute. La pression à cette surface est fixée à une atmosphère.La face opposée est adiabatique et imperméable, excluant tout flux thermique ou échange gazeux.Ce cas-test ne tient pas compte des effets mécaniques (déformations et contraintes). Cest précisément lune des limitations qui motive le développement du cas-test Ablation Test-case 4.0 intégrant le couplage pyromécanique afin de mieux représenter le comportement du matériau.Les résultats analysés concernent lévolution de la température, la progression de la pyrolyse ainsi que les réponses mécaniques associées. Ces travaux sappuient sur le logiciel open source PATO, basé sur OpenFOAM, permettant le développement et la validation du modèle. Ils permettent ainsi de proposer un cadre cohérent pour la validation et la comparaison de modèles pyromécaniques.

Development of benchmarks for the validation of pyromechanical models for the pyrolysis community.

Gloire BIDEAU , Jean LACHAUD

Université de Bordeaux, I2M,UMR 5295, F-33400, Talence, France

Context and objectives

Pyrolysis phenomena are central to many high-temperature applications, such as thermal protection systems and biomass conversion. However, mechanical effects induced by pyrolysis, including shrinkage and internal stresses, remain insufficiently represented in existing numerical models.
In this context, this work focuses on the development of Ablation Test-case 4.0, an extension of the reference Ablation Test-case 1.0 incorporating pyromechanical effects. The study considers a one-dimensional isotropic TACOT ablative material sample to analyze thermal and mechanical responses during pyrolysis.
The developed model introduces pyromechanical coupling in order to better represent the material response during pyrolysis. The analyzed results include temperature evolution, pyrolysis progression, and the associated mechanical responses.
This work is carried out using **PATO**, an open-source toolbox based on **OpenFOAM**. The obtained numerical results will be shared with the community.

Heat and mass transfer model

Pyrolysis: $\frac{\partial \chi_{ij}}{\partial t} = (1-\chi_{ij}) A_{ij} \exp\left(-\frac{E_{ij}}{RT}\right) \quad \forall i \in [1, N_p], \forall j \in [1, P_i]$

Mass Conservation:

Gas phase $\partial_t(\varepsilon_i \langle \rho_g \rangle)^g + \nabla(\varepsilon_i \langle \rho_g \rangle^g \langle \upsilon_g \rangle^g) = \pi_{tot}$

Solid phase $\partial_t(\langle \rho_s \rangle) + \nabla(\langle \rho_s \rangle \langle \upsilon_s \rangle^s) = -\pi_{tot}$

Momentum Conservation:

Gas phase

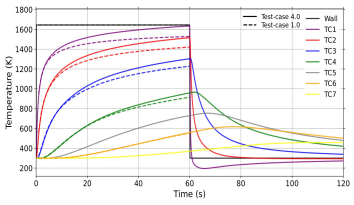
$$\partial_t\left(\frac{\varepsilon_g M_g}{R\langle T \rangle}\langle P_g \rangle^g\right) + \nabla\left(\frac{M_g}{R\langle T \rangle}\langle P_g \rangle^g\left[\frac{-K}{\mu_g}\nabla\langle P_g \rangle^g + \langle \upsilon_s \rangle^s\right]\right) = \pi_{tot}$$

$$\langle \upsilon_g \rangle^g = \frac{-K}{\varepsilon_g \mu_g}\nabla\langle P_g \rangle^g + \langle \upsilon_s \rangle^s$$

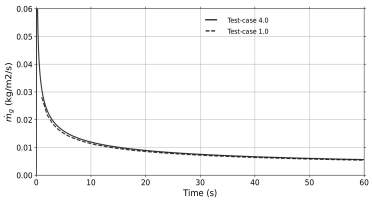
Energy Conservation:

$$\sum_{i\in[1,N_p]} \partial_t(\varepsilon_i \langle \rho_i \rangle^i \langle h_i \rangle^i) + \partial_t(\varepsilon_g \langle \rho_g \rangle^g \langle e_g \rangle^g) = \nabla(K \nabla \langle T \rangle)$$
$$-\nabla(\varepsilon_g \langle \rho_g \rangle^g \langle h_g \rangle^g \langle V_g \rangle^g)$$
$$-\nabla\Big(\sum_{i\in[1,N_p]} \varepsilon_i \langle \rho_i \rangle^i \langle h_i \rangle^i \langle V_s \rangle^s\Big)$$
$$-\sum_{i\in[1,N_p]} \langle h_i \rangle^i \partial_t(\varepsilon_i \langle \rho_i \rangle^i)$$

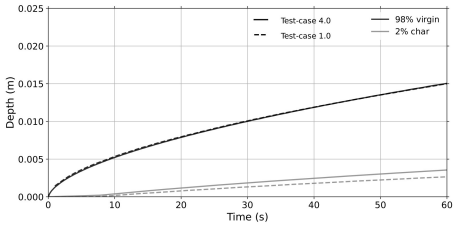
Results



Temperature evolution PATO/FIAT



Pyrolysis gas mass flux PATO/FIAT



Pyrolysis front propagation in TACOT PATO/FIAT

Mechanical response of solid phase

The nature of the thermo-pyro-mechanical coupling and the evolution of material properties are nonlinear, the problem is solved using a time-incremental formulation:

$$D^{n+1} = D^n + \Delta D$$

The solid phase of momentum conservation:

$\partial_t(\langle \rho_s \rangle \partial_t \langle u \rangle^s) - \nabla \langle \sigma \rangle^s = 0$ At the equilibrium: $\nabla \langle \delta\sigma_s \rangle^s = 0$

Deformation: $\langle \delta\varepsilon_s \rangle^s = \langle \delta\varepsilon^{el} \rangle^s + \langle \delta\varepsilon^{th} \rangle^s + \langle \delta\varepsilon^{pyr} \rangle^s$

Thermal expansion Strain: $\langle \delta\varepsilon^{th} \rangle^s = \alpha_s \langle \delta T \rangle^s$ Pyrolysis shrinkage Strain: $\langle \delta\varepsilon^{pyr} \rangle^s = \xi_s \langle \delta\tau \rangle^s$

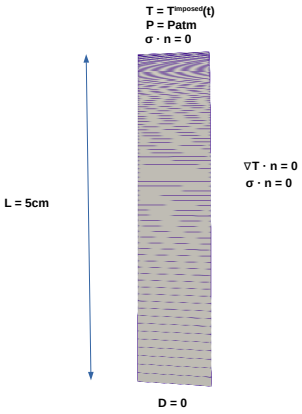
Hooke's law for isotropic material: $\sigma^{el} = \lambda tr(\varepsilon) I + 2\mu\varepsilon$

Total Stress Tensor:

$$\langle \sigma_s \rangle^s = \lambda tr\left(\langle \varepsilon^s \rangle^s - \langle \varepsilon^{th} \rangle^s - \langle \varepsilon^{pyr} \rangle^s\right) + 2\mu\left(\langle \varepsilon^s \rangle^s - \langle \varepsilon^{th} \rangle^s - \langle \varepsilon^{pyr} \rangle^s\right)$$

Simulation results (PATO)

Ablation Test-case 4.0 (1D)



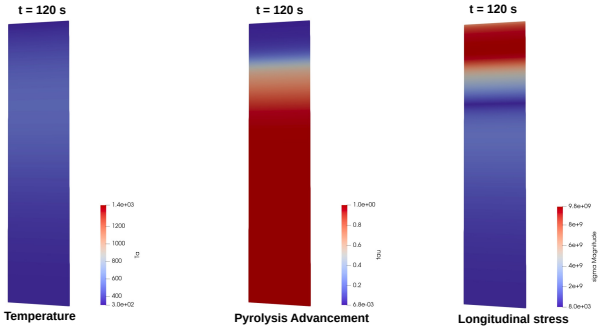
Time(second)	Temperature(Kelvin)
0s	300K
0.1s	1644K
60s	1644K
60.1s	300K
120s	300K

Temperature imposed at the TOP

	Virgin material	Char
Young Modulus	70 GPa	20 GPa
Poisson Coefficient	0.3	0.3
Thermal expansion	$1*10^{-6}$ K^{-1}	$8*10^{-5}$ K^{-1}

Thermo-mechanical Properties: TACOT

Pyrolysis Shrinkage Coefficient: $\xi = 0.5$



References

[1] Lachaud, J. Pyrolysis Models and Simulation Tools: A Cross-Community Comparative Review Highlighting Open Challenges.
[2] Lahouze, F. Pyromechanics: A Solid Mechanics Approach to Deformation During Pyrolysis.
[3] Landau, L. D., & Lifshitz, E. M. (1986). Theory of Elasticity. Elsevier.

Modeling of the Søderberg Electrode

Rachih Azeddine, Eramet Ideas

Submerged-arc furnaces producing ferromanganese (FeMn) drive 100150 kA through three self-baking Søderberg electrodes, each dissipating tens of MW. Locating the baking isotherm (773 K) inside the column is critical: too low risks paste breakthrough; too high wastes thermal energy and accelerates casing consumption. Since thermocouples survive only on the outer casing, modeling is the only window onto the internal current density and temperature fields.This work presents soderbergFoam, a custom OpenFOAM (Foundation v13) solver for the coupled electro-thermal problem in a Søderberg electrode. The steady-state, axisymmetric formulation couples current continuity and energy conservation through a temperature-dependent electrical conductivity (T), a mass-conserving slipping velocity, and the latent heat of baking absorbed across a mushy band. Four cellZones (paste, mixed compound, casing, clamps) capture the multi-material structure; outer-wall Robin boundary conditions and a volumetric induction source close the model.The solver agrees with a reference ANSYS Fluent case and with multi-campaign thermocouple data from an operating FeMn furnace. It is now used in-house at Eramet to test current, slipping-rate, and paste-formulation scenarios before plant trials

9th FOAM-U Conference · Bordeaux · 3-4 June 2026

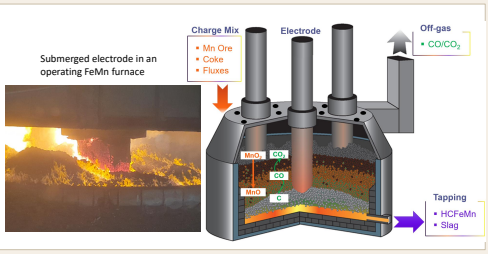
Modeling of the Søderberg Electrode

A coupled electro-thermal solver in OpenFOAM for FeMn furnace electrodes

PhD. Azeddine Rachih · *Senior Modeling Engineer* · *Eramet Ideas*

1 Industrial Context

Submerged-arc furnaces (SAFs) producing ferromanganese (FeMn) draw very high currents of **100-150 kA** through three Søderberg electrodes, dissipating 30-80 MW per furnace into the reduction reactions that convert Mn-rich ores into alloys for steelmaking.



FeMn submerged-arc furnace : the three electrode columns descending through the burden to the smelting zone.

2 The Søderberg Electrode

Self-baking electrodes are continuously consumed at the tip and re-formed at the top: **green paste** is poured cold into a sheet-steel casing fitted with internal steel fins, then progressively heated by Joule and induction effects as it descends, passing through softening, pyrolysis and finally graphitisation before being consumed at the arc.

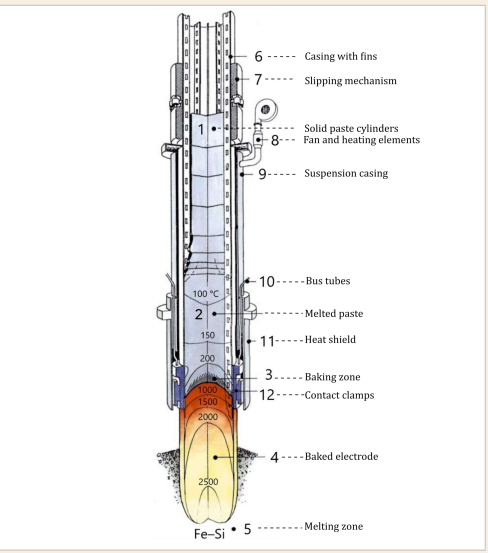


Illustration of a Søderberg electrode column, courtesy of Elkem Carbon : paste path from casing (top) through air-heating, baking and arc zones.

3 Why Model It?

- **Locate the baking isotherm (≈ 773 K)** → too low risks paste breakthrough; too high wastes thermal energy and accelerates casing consumption.
- **Predict response to operational changes** → current intensity, slipping rate, paste formulation, casing geometry, fins arrangement, before committing capital.
- **Access internal fields that resist instrumentation** → thermocouples survive only on the casing, the model is the sole window onto current density, temperature and σ(T) inside the active volume.
- **Provide an inexpensive surrogate for campaign optimisation** and root-cause analysis of electrode breakage incidents.

Typical operating envelope

Electrode current I	**136 kA**
Slipping rate	**24.4 mm / h**
Arc tip temperature	**2000 K**
Inlet paste temperature	**323 K**
Electrode radius	**0.95 m**
Modelled length	**5.70 m**

4 Coupled Electro-Thermal Model

Steady-state, axisymmetric (5° wedge). The electric potential φ and temperature T are coupled through σ(T) and the volumetric Joule source.

Current continuity

$$\nabla \cdot (\sigma(T)\, \nabla\varphi) = 0$$

Energy (advection–diffusion–source)

$$\nabla \cdot (\rho\, C_p\, U\, T) - \nabla \cdot (k\, \nabla T) = Q_j + Q_{ind} - \rho\, L\, \partial f_s/\partial T \cdot U \cdot \nabla T$$

Joule heat

$$Q_j = \sigma(T)\, |\nabla\varphi|^2$$

Mass-conserving slipping velocity

$$U(T) = u_{slip} \cdot \rho_{baked} / \rho(T) \qquad \text{(paste / mixed)}$$

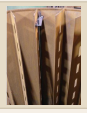
5 Multi-zone Material Model

Four cellZones: **paste**, **mixed compound** (paste + steel fins), **casing** (steel), **clamps** (Cu). σ(T), k(T), Cp(T) piecewise-linear, with latent heat (200 kJ/kg) absorbed across the [673, 873] K mushy band.

Mixed-compound rule (fin-area derived):

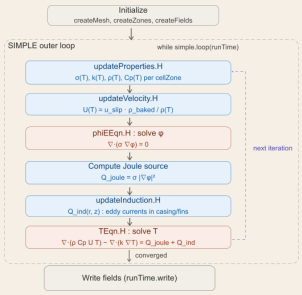
$$X_mix = (1 - \alpha\, p_steel)\, X_paste + \alpha\, p_steel\, X_steel$$

$$p_steel = \rho_steel\, A_fins\, /\, (\rho_steel\, A_fins + \rho_paste\, A_paste)$$



6 OpenFOAM Implementation

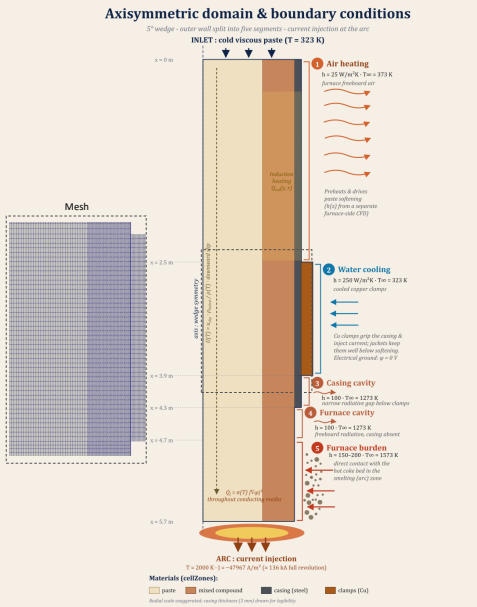
Custom solver `soderbergFoam` (Foundation v13). Outer SIMPLE loop couples φ and T. σ(T) and U(T) refreshed every iteration. Cell zones built by `topoSet`; current injection on the arc patch as `codedMixed` with refGrad = −J/σ_face for a constant-current condition (~136 kA full revolution). Outer-wall heat transfer as Robin BCs with per-segment (h, T∞) calibrated from the air-heating sub-model.



7 Supporting Sub-models

- **Paste softening / rheology** : viscous-paste descent model upstream of the baking zone; sets the inlet density and slip boundary conditions.
- **Air-heating coefficient** : separate furnace-side CFD provides the convective h(z) extracted along the casing outer surface, used as the Robin BC here.
- **Induction heating** : proximity of current bars to the casing modeled as a volumetric eddy-current source with axial + radial exponential decay.

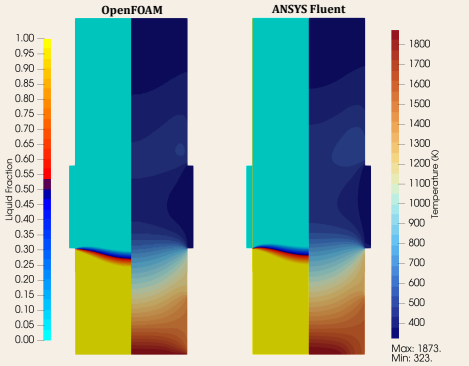
8 Mesh & Boundary Setup



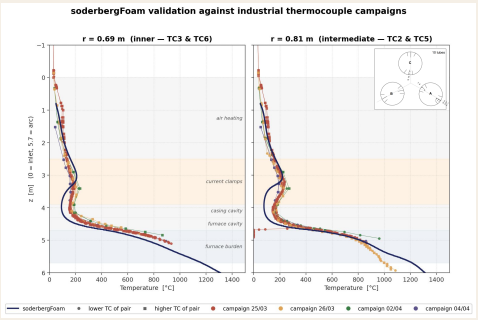
Mesh & BC : four cellZones (paste, mixed compound, casing, clamps), ~21 000 hex cells. Inlet (top), arc outlet (bottom), 5 outer-wall Robin BCs.

9 Validation

Cross-validation against a **reference Fluent case** and against **industrial thermocouple campaigns** (TC at r = 0.93 m, multiple campaigns).

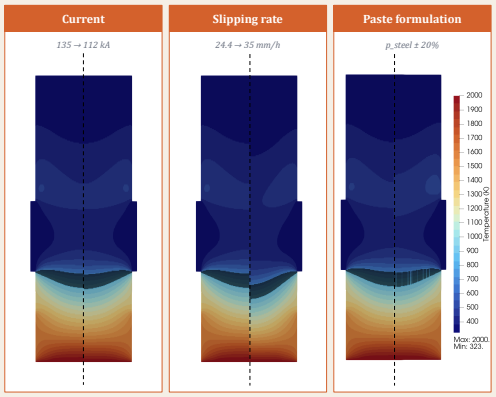


Validation of soderbergFoam against ANSYS Fluent for Søderberg electrode baking. Each panel shows liquid fraction (left half) and temperature (right half); the paste-to-carbon transition front is captured at the same axial position by both solvers.



soderbergFoam vs. industrial thermocouple data at r = 0.69 m (TC3/TC6, left) and r = 0.81 m (TC2/TC5, right) over four campaigns (25/03 and 04/04).

10 What-if Scenarios



11 Take-aways

- **An OpenFOAM solver for the coupled electro-thermal problem in a self-baking electrode**, with temperature-dependent conductivity, latent heat of baking, and induction heating treated explicitly.
- **Agrees with the Fluent reference case and with plant thermocouple readings**; the implementation is open and maintained in-house at Eramet.
- **Lets operational and design changes be tested numerically before committing to a plant trial.**

12 Next Steps

- **Couple to a furnace-side CFD model** so the air-heating boundary condition becomes self-consistent rather than imposed from an offline extraction.
- **Move from steady state to transient operation**, slipping changes, current ramps, off-spec paste batches, using the converged steady field as initial condition.
- **Extend to 3-D to resolve inter-electrode coupling and non-axisymmetric paste distribution.**
- **Release the solver publicly to support OpenFOAM work in electrometallurgy.**

eramet
COMMITTED TO SUSTAINABLE METALS

Save contact

Acknowledgments
This work has been accomplished thanks to the past and present members of the Eramet Ideas modeling team, in particular A. Nigmetova, B. Laboudigue, C. Gouny, H. Han, O. Yani. As well as SINTEF and Eramet Norway team who provided the electromagnetic induction model and the measurements.

Selected references
[1] O. Yani Søderberg Electrode Modeling: Simulation of Electrode Paste Softening and Baking (Eramet, 2025).
[2] OpenFOAM Foundation v13 source.
[3] B. Larsen. Electrode Models For Søderberg Electrodes.

Partner Institutions and Sponsors

Institutions

We gratefully acknowledge ENSAM and Université de Bordeaux for their support.

Sponsors

We gratefully acknowledge HyFAR-ARA for its support. HyFAR-ARA is a scientific association that federates public institutions, research and educational organisations, and industrial companies interested in hypersonic systems and their applications.